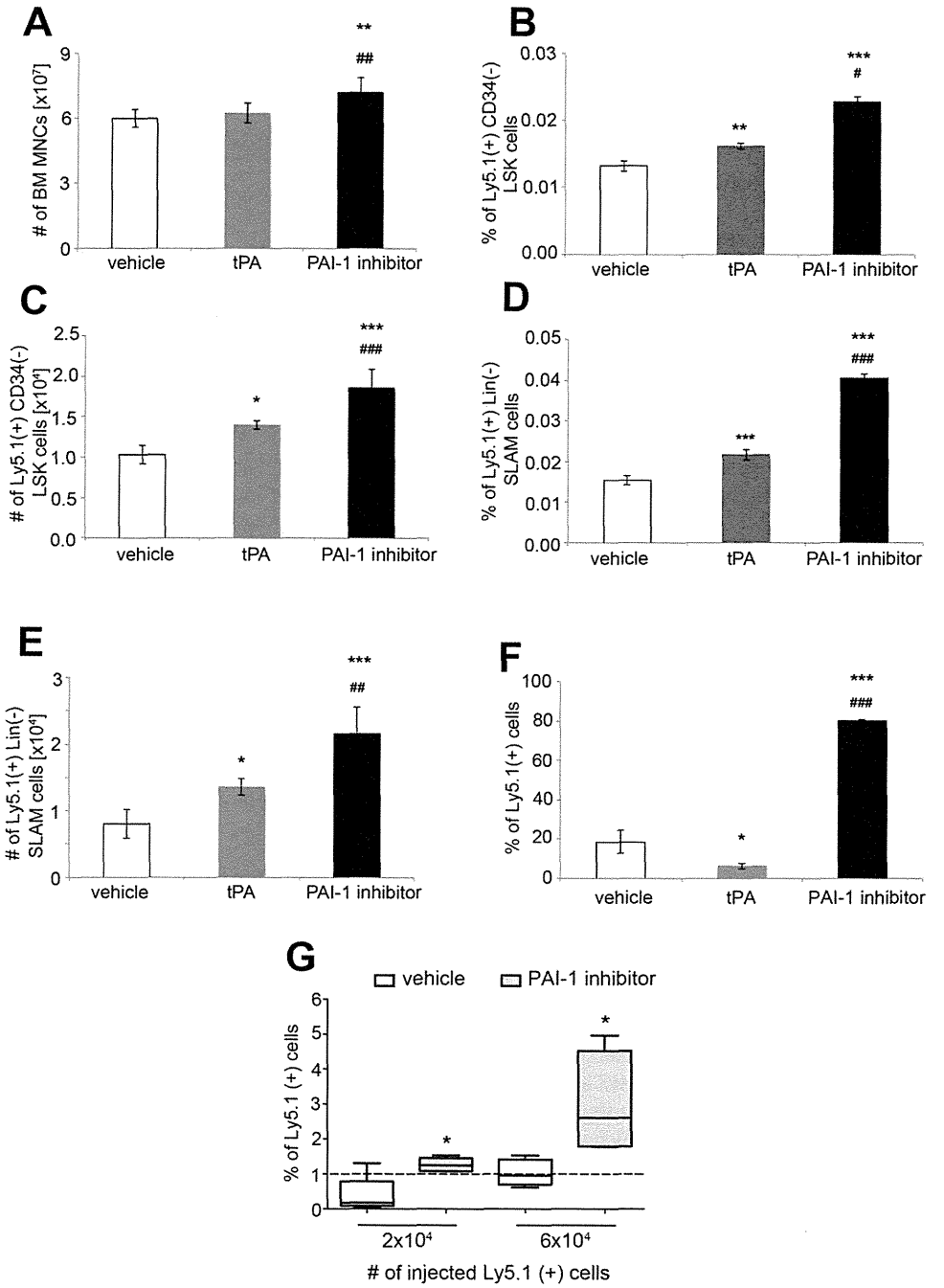

Figure 7. The PAI-1 inhibitor enhances the self-renewal capacity of hematopoietic stem cells. **(A–E):** The Ly5.2$^+$ mice were exposed to 9 Gy radiation, followed by transplantation with 2.5 × 10^6 Ly5.1$^+$ BM MNCs. They were administered the vehicle, tPA, or the PAI-1 inhibitor daily for 5 consecutive days. BM MNCs were collected 15 weeks after transplantation. BM MNCs were obtained from four long leg bones per mouse, and were pooled for the analysis of (A) the total number of donor-derived Ly5.1$^+$ BM MNCs, (B) the proportion of CD34$^-$LSK cells among Ly5.1$^+$ cells, (C) the total number of CD34$^-$LSK cells, (D) the proportion of Lin$^-$SLAM cells among Ly5.1$^+$ cells, (E) the total number of Lin$^-$SLAM cells. The data from four independent experiments are shown ($n = 12$ for each condition). *, $p < .05$; **, $p < .01$; ***, $p < .001$ versus the vehicle group; $^{\#}$, $p < .05$; $^{\#\#}$, $p < .01$; $^{\#\#\#}$, $p < .001$ versus the tPA group. The p value was calculated by one-way ANOVA followed by Bonferroni post-test. **(F):** The chimerism of donor-derived Ly5.1$^+$ cells in the secondary recipients. Donor-derived Ly5.1$^+$ BM MNCs (1 × 10^6) in the primary recipient mice were retransplanted, together with 5 × 10^5 Ly5.2$^+$ competitor cells, into the 9 Gy-irradiated Ly5.2$^+$ secondary recipient mice. BM cells were analyzed 12 weeks after the secondary transplantation. The data from three independent experiments are shown ($n = 10$ for each condition). *, $p < .05$; ***, $p < .001$ versus the vehicle group; $^{\#\#\#}$, $p < .001$ versus the tPA group. **(G):** The chimerism of a small number of donor-derived Ly5.1$^+$ cells in the secondary recipients. A total of 2 × 10^4 or 6 × 10^4 Ly5.1$^+$ BM cells from the primary recipient mice, with 5 × 10^5 Ly5.2$^+$ competitor cells, were transplanted into the 9 Gy-irradiated Ly5.2$^+$ secondary recipient mice. Twelve weeks after the secondary transplantation, the chimerism of donor cells in the BM was evaluated. The boxes in white and gray represent the chimerism of donor-derived Ly5.1$^+$ cells in the vehicle- and PAI-1 inhibitor-treated mice, respectively. The horizontal lines in the box represent the median chimerism, and bars indicate the SD. The dashed line indicates the cut-off value (1%). Data from two independent experiments are shown ($n = 5$ for each condition). *, $p < .05$ versus the vehicle group. Abbreviations: BM, bone marrow; MNC, mononucleic cell; PAI-1, plasminogen activator inhibitor-1; tPA, tissue-type plasminogen activator.

regeneration, Galipeau and colleagues have demonstrated that mesenchymal stem cells (MSCs) derived from PAI-1 KO mice exhibited higher regenerative potential than those from WT mice [30]. Furthermore, chemical manipulation of the PAI-1 activity improves the engraftment of MSCs, defining PAI-1 as a negative regulator of transplanted stem cell survival in vivo [30]. This study clarified the active involvement of PAI-1 in the hematopoietic regeneration after irradiation.

Proper treatment of the initial stage of hematopoietic recovery and the prevention of premature HSC exhaustion could therefore significantly improve the clinical outcome of transplantation [1, 2]. In this regard, our study demonstrated that, despite a short period of administration, the suppression of the PAI-1 activity by a low molecular weight compound could induce both rapid hematopoietic regeneration through increased cycling of HSCs and expansion of the long-term HSCs. This opens a new avenue for improving HSCT. It should be emphasized that the PAI-1 inhibitor does not induce HSC exhaustion or malignancy in spite of its potent ability to increase the cycling of HSCs. The results of this study clearly demonstrated that c-kit$^+$ HSPCs in the group treated with the PAI-1 inhibitor preferentially localized to the BM niche, just like in the vehicle-treated group, suggesting that the interaction between the hematopoietic progenitor cells and niche is maintained even after the treatment with a PAI-1 inhibitor. This may be a plausible explanation for why the PAI-1 inhibitor does not induce HSC exhaustion.

Both the PAI-1 inhibitor and tPA theoretically activate the fibrinolytic pathway and the subsequent hematopoietic regeneration, but their effects in vivo in animals appear to be different. This is partly explained by the differences in the routes of administration between tPA and the PAI-1 inhibitor, as well as the doses, mechanisms of action, and/or half-lives of these agents. Recombinant tPA is administered intravenously (a large amount of tPA is given directly into the circulation), and immediately activates the fibrinolytic pathway, but its half-life is only a few minutes [17]. In contrast, the PAI-1 inhibitor was given orally, and was absorbed in the gut, entered into the circulation gradually, inhibited the PAI-1 moiety, and subsequently upregulated the tPA activity leading to its effects on the fibrinolytic pathway. The half-life of the PAI-1 inhibitor is much longer (6.5 hour) than that of tPA.

It is also important to note that tPA administration itself increased the PAI-1 level, suggesting a potential negative feedback effect in this pathway and limits to the therapeutic benefits of tPA for hematopoietic regeneration. In addition, the repopulating capacity of HSCs in tPA-treated mice showed a slight decrease, suggesting that tPA treatment may induce HSC exhaustion. It should also be mentioned that PAI-1 regulates not only tPA, but also other proteins (i.e., vitronectin, urokinase-type plasminogen activator (uPA), and low density lipoprotein receptor (LDLR)) [5, 31, 32] and thereby has an impact on broader biological systems.

Conclusion

In conclusion, our study provides the first direct evidence that PAI-1 is a negative regulator of hematopoietic regeneration, and that the inhibition of PAI-1 activity, either genetically or by a low molecular weight compound, significantly improves donor-derived hematopoiesis after transplantation. Our findings give new insights into the treatment of HSCT and for clinical transplantation medicine.

Acknowledgments

We appreciate the help of Dr. Koichi Hattori (Institute of Medical Science, University of Tokyo, Japan) for kindly providing the tPA KO mice. We thank Dr. Nobuo Watanabe (Tokai University School of Medicine, Japan) for helpful discussion and wrote the manuscript. We also thank the members of the Research Center for Regenerative Medicine of Tokai University, especially Tomomi Takanashi, Kozue Hiyama, and Tomoko Uno, for the technical support. We thank the members of the Animal Care Center of Tokai University for their meticulous care of the experimental animals. This work was supported by Japanese Grants-in-Aid for Scientific Research from the Ministry of Education, Culture, Sports, Science and Technology (MEXT), from the Ministry of Health, Labor and Welfare (MHLW), from the National Institute of Biomedical Innovation (NIBIO), from the Japan Science and Technology Agency (JST), and from the Tokai University School of Medicine Research Aid. Special thanks are due to the MARA Education Foundation, Malaysia, for supporting the scholarship awarded to A.A.I.

Author Contributions

A.A.I.: collection and assembly of data, data analysis and interpretation, and manuscript writing; T.Y.: conception and design, data analysis and interpretation, manuscript writing, and financial support; M.O.: data analysis and interpretation; T.D.: provision of study material; C.v.Y.d.S.: manuscript writing; T.M.: provision of study material, data analysis and interpretation, and manuscript writing; K.A.: conception and design, data analysis and interpretation, financial support, and final approval of manuscript.

Disclosure of Potential Conflicts of Interest

The authors indicate no potential conflicts of interest.

References

1 Perumbeti A, Sacher RA. Hematopoietic Stem Cell Transplantation. Available at http://emedicine.medscape.com/article/208954. Accessed November 30, 2012.

2 Chawla R, Davies HD. Infections After Bone Marrow Transplantation. Available at http://emedicine.medscape.com/article/1013470. Accessed September 13, 2012.

3 Kolev K, Machovich R. Molecular and cellular modulation of fibrinolysis. Thromb Haemost 2003;89:610–621.

4 Collen D, Lijnen HR. Basic and clinical aspects of fibrinolysis and thrombolysis. Blood 1991;78:3114–3124.

5 Diebold I, Kraicun D, Bonello S et al. The 'PAI-1 paradox' in vascular remodeling. Thromb Haemost 2008;100:984–991.

6 Heissig B, Lund LR, Akiyama H et al. The plasminogen fibrinolytic pathway is required for hematopoietic regeneration. Cell Stem Cell 2007;1:658–670.

7 Heissig B, Ohki M, Ishihara M et al. Contribution of the fibrinolytic pathway to hematopoietic regeneration. J Cell Physiol 2009;221:521–525.

8 Izuhara Y, Takahashi S, Nangaku M et al. Inhibition of plasminogen activator inhibitor-1: Its mechanism and effectiveness on coagulation and fibrosis. Atertio Thromb Vasc Biol 2008;28:672–677.

9 Yamaoka N, Kodama H, Izuhara Y et al. Structure-activity relationships of new N-acylanthranilic acid derivatives as plasminogen activator inhibitor-1 inhibitors. Chem Pharm Bull (Tokyo) 2011;59:215–224.
10 Izuhara Y, Yamaoka N, Kodama H et al. A novel inhibitor of plasminogen activator inhibitor-1 provides antithrombotic benefits devoid of bleeding effect in nonhuman primates. J Cereb Blood Flow Metab 2010;30: 904–912.
11 Carmeliet P, Kieckens L, Schoonjans L et al. Plasminogen activator inhibitor-1 gene-deficient mice. I. Generation by homologous recombination and characterization. J Clin Invest 1993;92:2746–2755.
12 Carmeliet P, Stassen JM, Schoonjans L et al. Plasminogen activator inhibitor-1 gene-deficient mice. II. Effects on hemostasis, thrombosis, and thrombolysis. J Clin Invest 1993;92:2756–2760.
13 Carmeliet P, Schoonjans L, Kieckens L et al. Physiological consequences of loss of plasminogen activator gene function in mice. Nature 1994;368:419–424.
14 Nilsson SK, Johnston HM, Coverdale JA. Spatial localization of transplanted hemopoietic stem cells: Inferences for the localization of stem cell niches. Blood 2001;97:2293–2299.
15 Yahata T, Muguruma Y, Yumino S et al. Quiescent human hematopoietic stem cells in the bone marrow niches organize the hierarchical structure of hematopoiesis. Stem Cells 2008;26:3228–3236.
16 Zhang B, Ho YW, Huang Q et al. Altered microenvironmental regulation of leukemic and normal stem cells in chronic myelogenous leukemia. Cancer Cell 2012;21:577–592.
17 Narita M, Bu G, Herz J et al. Two receptor systems are involved in the plasma clearance of tissue-type plasminogen activator (t-PA) in vivo. J Clin Invest 1995;96:1164–1168.
18 Na Nakorn T, Traver D, Weissman IL et al. Myeloerythroid-restricted progenitors are sufficient to confer radioprotection and provide the majority of day 8 CFU-S. J Clin Invest 2002;109:1579–1585.
19 Jaroscak J, Goltry K, Smith A et al. Augmentation of umbilical cord blood (UCB) transplantation with ex vivo-expanded UCB cells: Results of a phase 1 trial using the AastromReplicell System. Blood 2003;101:5061–5067.
20 Ando K, Yahata T, Sato T et al. Direct evidence for ex vivo expansion of human hematopoietic stem cells. Blood 2006;107:3371–3377.
21 Dahlberg A, Delaney C, Bernstein ID. Ex vivo expansion of human hematopoietic stem and progenitor cells. Blood 2011;117: 6083–6090.
22 Rao JS, Rayford A, Yamamoto M et al. Modulation of fibrinolysis by ionizing radiation. J Neurooncol 1994;22:161–171.
23 Zhao W, O'Malley Y, Robbins ME. Irradiation of rat mesangial cells alters the expression of gene products associated with the development of renal fibrosis. Radiat Res 1999;152:160–169.
24 Milliat F, Sabourin JC, Tarlet G et al. Essential role of plasminogen activator inhibitor type-1 in radiation enteropathy. Am J Pathol 2008;172:691–701.
25 Rubin P. Law and order of radiation sensitivity. Absolute versus relative. Front Radiat Ther Oncol 1989;23:7–40.
26 Sugrue T, Lowndes NF, Ceredig R. Mesenchymal stromal cells: Radio-resistant members of the bone marrow. Immunol Cell Biol 2013;91:5–11.
27 Czekay RP, Wilkins-Port CE, Higgins SP et al. PAI-1: An Integrator of Cell Signaling and Migration. Int J Cell Biol 2011;2011: 562481.
28 Chan JC, Duszczyszyn DA, Castellino FJ et al. Accelerated skin wound healing in plasminogen activator inhibitor-1-deficient mice. Am J Pathol 2001;159:1681–1688.
29 Bergheim I, Guo L, Davis MA et al. Critical role of plasminogen activator inhibitor-1 in cholestatic liver injury and fibrosis. J Pharmacol Exp Ther 2006;316:592–600.
30 Copland IB, Lord-Dufour S, Cuerquis J et al. Improved autograft survival of mesenchymal stromal cells by plasminogen activator inhibitor 1 inhibition. Stem Cells 2009;27: 467–477.
31 Balsara RD, Ploplis VA. Plasminogen activator inhibitor-1: The double-edged sword in apoptosis. Thromb Haemost 2008;100:1029–1036.
32 Herz J, Strickland DK. LRP: A multifunctional scavenger and signaling receptor. J Clin Invest 2001;108:779–784.


See www.StemCells.com for supporting information available online.

STEM CELLS®

TISSUE-SPECIFIC STEM CELLS

Stage-Specific Roles for Cxcr4 Signaling in Murine Hematopoietic Stem/Progenitor Cells in the Process of Bone Marrow Repopulation

CHEN-YI LAI,[a,b] SATOSHI YAMAZAKI,[a] MOTOHITO OKABE,[a] SACHIE SUZUKI,[a] YOSHIHIRO MAEYAMA,[c] YASUAKI IIMURA,[d] MASAFUMI ONODERA,[e] SHIGERU KAKUTA,[f,g] YOICHIRO IWAKURA,[f,h] MASANORI NOJIMA,[i] MAKOTO OTSU,[a,b] HIROMITSU NAKAUCHI[a]

[a]Division of Stem Cell Therapy, [b]Stem Cell Bank, Center for Stem Cell Biology and Regenerative Medicine, [f]Laboratory of Molecular Pathogenesis, Center for Experimental Medicine and Systems, and [i]Division of Advanced Medicine Promotion, Advanced Clinical Research Center, Institute of Medical Science, University of Tokyo, Tokyo, Japan; [c]Upper GI Surgery Division, Department of Surgery, Hyogo College of Medicine, Kobe, Japan; [d]Kushiro City General Hospital, Kushiro, Japan; [e]Department of Genetics, National Research Institute of Child Health and Development, Tokyo, Japan; [g]Department of Biomedical Science, Graduate School of Agricultural and Life Sciences, University of Tokyo, Japan; [h]Division of Experimental Animal Immunology, Research Institute for Biomedical Sciences/Graduate School of Biological Science, Tokyo University of Science, Tokyo, Japan

Correspondence: Makoto Otsu, Ph.D., M.D., Stem Cell Bank and Division of Stem Cell Therapy, Center for Stem Cell Biology and Regenerative Medicine, Institute of Medical Science, University of Tokyo, 4-6-1 Shirokanedai, Minato-ku, 108-8639 Tokyo, Japan. Telephone: +81-3-6409-2342; Fax: +81-3-6409-2343; e-mail: motsu@ims.u-tokyo.ac.jp; or Hiromitsu Nakauchi, Ph.D., M.D., Division of Stem Cell Therapy, Center for Stem Cell Biology and Regenerative Medicine, Institute of Medical Science, University of Tokyo, 4-6-1 Shirokanedai, Minato-ku, 108-8639 Tokyo, Japan. Telephone: +81-3-5449-5330; Fax: +81-3-5449-5451; e-mail: nakauchi@ims.u-tokyo.ac.jp

Received October 17, 2013; accepted for publication January 28, 2014; first published online in STEM CELLS *EXPRESS* February 8, 2014.

1066-5099/2014/$30.00/0

http://dx.doi.org/10.1002/stem.1670

Key Words. Chemokine receptors • Hematopoietic stem cells (stem and primitive progenitor cells) • Stem cell transplantation • Gene therapy (gene transfer to hematopoietic stem cells)

ABSTRACT

Hematopoietic cell transplantation has proven beneficial for various intractable diseases, but it remains unclear how hematopoietic stem/progenitor cells (HSPCs) home to the bone marrow (BM) microenvironment, initiate hematopoietic reconstitution, and maintain life-long hematopoiesis. The use of newly elucidated molecular determinants for overall HSPC engraftment should benefit patients. Here, we report that modification of C-X-C chemokine receptor type 4 (Cxcr4) signaling in murine HSPCs does not significantly affect initial homing/lodging events, but leads to alteration in subsequent BM repopulation kinetics, with observations confirmed by both gain- and loss-of-function approaches. By using C-terminal truncated Cxcr4 as a gain-of-function effector, we demonstrated that signal augmentation likely led to favorable in vivo repopulation of primitive cell populations in BM. These improved features were correlated with enhanced seeding efficiencies in stromal cell cocultures and altered ligand-mediated phosphorylation kinetics of extracellular signal-regulated kinases observed in Cxcr4 signal-augmented HSPCs in vitro. Unexpectedly, however, sustained signal enhancement even with wild-type Cxcr4 overexpression resulted in impaired peripheral blood (PB) reconstitution, most likely by preventing release of donor hematopoietic cells from the marrow environment. We thus conclude that timely regulation of Cxcr4/CXCR4 signaling is key in providing donor HSPCs with enhanced repopulation potential following transplantation, whilst preserving the ability to release HSPC progeny into PB for improved transplantation outcomes. STEM CELLS *2014;32:1929–1942*

INTRODUCTION

Hematopoietic stem cells (HSCs) have been used in transplantation to treat various intractable disorders [1–3]. Hematopoietic reconstitution is considered to be a process that can be divided into three major steps: (a) a homing/lodging step where HSCs transmigrate into the bone marrow (BM) cavity; (b) a BM repopulation step where HSCs replicate themselves while producing progenitor cells with multilineage differentiation potential; (c) a peripheral reconstitution step where mature cells are released from BM. Failure in any of these processes could impair transplantation outcomes [4].

HSC behavior is thought tightly regulated by certain extrinsic factors within the BM microenvironment (niche) [5]. HSC fate after transplantation may also be affected by similar external cues but much remains unclarified. We here focused on stromal cell-derived factor 1 (SDF-1)/CXCL12, abundant in BM [6]. The C-X-C chemokine receptor type 4 (CXCR4), a receptor for SDF-1/CXCL12, plays a role in hematopoiesis [7–9]. Knockout (KO) mouse studies have demonstrated the importance of the Sdf-1/Cxcr4 axis in HSCs in both fetal [10] and adult hematopoiesis, with a critical role in the latter identified for maintenance of HSC dormancy [7, 8, 11]. CXCR4 signaling has also been implicated in transplantation of adult hematopoietic stem and progenitor cells (HSPCs), as blockage of the SDF-1/CXCR4 axis in human HSPCs before transplantation compromised their engraftment/repopulation in Nonobese diabetic/Severe combined immunodeficiency (NOD/SCID) mice [12]. Similarly poor hematopoietic reconstitution was observed following transplantation of *Cxcr4*-KO mouse BM cells [7, 8]. In contrast, overexpression of CXCR4 in human HSPCs led to enhanced engraftment in mouse BM, suggesting that this modification might benefit transplanted patients [13, 14].

In this study, to determine the precise role of Cxcr4 signaling, highly purified murine HSCs and their progenies were used in both gain-of-function (overexpression) and loss-of-function (KO or desensitization) approaches. In

semiquantitative analysis of gain-of-function effects, we used not only wild-type (WT) Cxcr4-overexpressing cells but also cells expressing Cxcr4 with a specific C-terminal deletion (ΔC) homologous to that found in patients with the disorder termed warts, hypogammaglobulinemia, infections, and myelokathexis (WHIM) syndrome [15], for which a mouse model has recently been developed [16]. This truncation is regarded as a gain-of-function mutation, because it increases cell-surface stability of CXCR4 without impairing CXCR4 signaling capabilities [16–20]. By using this combinational approach, we assessed each of the multiple steps in donor cell reconstitution in mice that received Cxcr4-modified HSC/HSPCs and dissected stage-specific roles that Cxcr4 signaling plays in transplanted cells.

Materials and Methods

Mouse HSCs and HSPCs

C57BL/6 (B6)-Ly5.1 mice came from Sankyo Labo Service (Tokyo, http://www.sankyolabo.co.jp). B6-Ly5.2 and enhanced green fluorescent protein (EGFP)-transgenic (Tg) (CAG-EGFP) mice were from Japan SLC (Shizuoka, http://www.jslc.co.jp). Generation of *Cxcr4*-KO mice and of Kusabira Orange (KuO)-Tg mice is described in Supporting Information Methods [21–25]. Purified murine $CD34^{neg/low}$ c-$Kit^+Sca\text{-}1^+$Lineage marker-negative ($CD34^-$KSL) cells were used as the HSC source [26, 27]. Where indicated, KSL cells (referred to as HSPCs) were used. Considering the status of cells, that is, either fresh or postexpansion, we defined $CD34^-$KSL cells as fresh HSCs or cultured HS(P)Cs and defined KSL cells as fresh HSPCs or cultured HSPCs. Cell sorting was performed on a MoFlo cytometer (Beckman Coulter, Brea, CA, https://www.beckmancoulter.com) or a FACSAria II (BD Biosciences, San Diego, CA, http://www.bdbiosciences.com). The Institutional Animal Care and Use Committee, University of Tokyo, approved all animal experiments.

Retrovirus Transduction of HSC/HSPCs

The pGCDNsam-IRES-EGFP (DNsam-I/E) [25] was used as a control retroviral vector (Mock). Murine WT-*Cxcr4* cDNA was used to construct DNsam-WT-Cxcr4-I/E. We constructed DNsam-ΔC-Cxcr4-I/E, harboring mutant cDNA that mimics the type of mutation most frequent in WHIM syndrome [15, 18]. Production of VSV-G-retroviruses is described [25, 28, 29]. HSC/HSPCs were transduced with retrovirus as described [25]. Three days after transduction, cells expressing EGFP ($EGFP^+$ cells) were sorted and subjected to downstream assays (Supporting Information Fig. S1A).

Migration, Cell Proliferation, and Single-Cell Colony Assays in Liquid Culture

Chemotactic response toward SDF-1/CXCL12 was tested in $EGFP^+$ cultured HS(P)Cs [30]. Our single-cell colony assay in liquid medium is described [26, 31, 32]. Colonies were evaluated at days 11 and 14 for gain-of-function and loss-of-function studies, respectively (Supporting Information).

Assessment of Seeding Efficiency in Stromal Cell Coculture

The ability to repopulate an irradiated stromal cell layer was tested in sorted $EGFP^+$ HS(P)Cs or fresh HSCs using the in vitro coculture assay [33] that we developed from cobblestone-like area formation assays [34, 35] and is similar to a system recently shown to be useful to assess HSCs' clonogenic ability in stromal cocultures at a clonal level [36]. Test cells were sorted onto irradiated (50 Gy) C3H10T1/2 stromal cell layers pre-established in six-well plates containing Minimum Essential Medium Eagle Alpha in the presence of mouse stem cell factor (mSCF), mouse Thrombopoietin (mTPO), human Erythropoietin (hEPO), and mouse Interleukin-3 (mIL-3). Formed cobblestone-like areas were counted as described (Supporting Information).

HSPC Homing Assay

$EGFP^+$ cultured HSPCs (test cells) were cotransplanted into irradiated recipients with either fresh KSL or total BM cells from KuO-Tg mice (reference cells) numbered as shown. To desensitize HSPCs to SDF-1, fresh KuO-expressing (KuO^+) KSL cells preincubated with AMD3100 [37–39] (test cells) were cotransplanted into irradiated recipients with total BM cells from EGFP-Tg mice (reference cells). At the times indicated, both $EGFP^+$ and KuO^+ cells were counted in the same BM samples using flow cytometry analysis. Homing events were represented by the ratio of test cells to reference cells (schematic representation, see Supporting Information Figs. S1B, S2A, S3).

Early HSPC Repopulation Kinetics in Recipient BM

We estimated homing (16 and 24 hours) and subsequent repopulation (days 2–6) by infused test cells by counting colony-forming cells (CFCs) in recipient BM. Test cells were transplanted alone into lethally irradiated mice. Cells obtained at indicated times from recipient bones were subjected to colony-forming assays and scored [33] (Supporting Information).

Competitive Repopulation Assays

To assess both short-term (2–3 weeks) and long-term (>16 weeks) reconstitution ability in test cells, a competitive repopulation assay was used [26]. The detailed protocol is described in Supporting Information.

Flow Cytometry Analyses

To assess intracellular phosphorylation kinetics of signaling molecules, cultured $EGFP^+$ HS(P)Cs were cytokine-starved and restimulated with SDF-1/CXCL12. Cells were stained with anti-phospho-extracellular signal-regulated kinases 1/2 (Erk1/2), anti-phospho-Akt, or isotype-control rabbit mAbs (Cell Signaling Technology, Beverly, MA, http://www.cellsignal.com), followed by Alexa Fluor 647-anti-rabbit IgG (Invitrogen, Carlsbad, CA, http://www.invitrogen.com). Details are shown in Supporting Information together with other flow cytometry analyses.

Statistical Analysis

All data are expressed as means ± SD. Comparisons between two groups were subjected to Student's unpaired *t* test using *Prism 4* software (GraphPad La Jolla, CA, http://www.graphpad.com), and comparisons of more than two groups were performed by Dunnett's multiple comparison (vs. control) unless otherwise annotated. p for trend was tested using polynomial contrast in general linear models. A level of $p < .05$ was considered significant.

Results

Stepwise Gain-of-Function Effects of Exogenous Cxcr4 on Transduced HS(P)Cs, with Greater Response for the ΔC-Type Receptor

We constructed a system for gain-of-function studies as detailed in Supporting Information. With this system, we

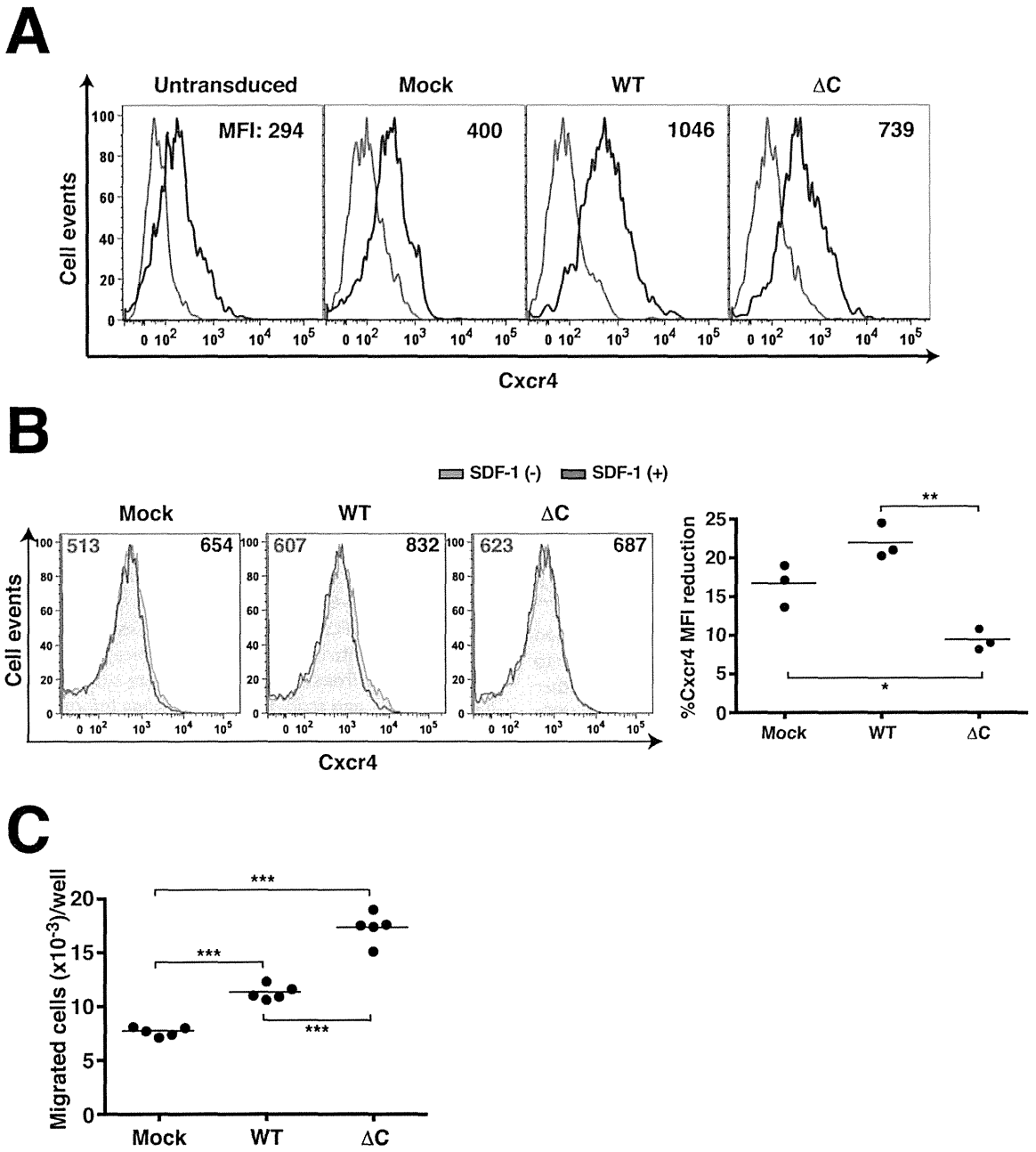

Figure 1. Rationale for gain-of-function experiments to assess role of C-X-C chemokine receptor type 4 (Cxcr4) signaling in murine hematopoietic stem/progenitor cells (HSPCs). **(A):** Assessment of cell surface Cxcr4 expression in HS(P)Cs after 1 week of cultivation following transduction and enhanced green fluorescent protein positive ($EGFP^+$) cell sorting. Cxcr4 intensity (blue histograms) represents endogenous Cxcr4 expression by untransduced cells (Untransduced) and Mock-transduced cells (Mock), or the sum of both endogenous and exogenous Cxcr4 expression by transduced cells (WT, ΔC). MFI values are shown. Red histogram: isotype control. **(B):** Receptor internalization. Cultured and sorted HS(P)Cs were left unstimulated or were stimulated with SDF-1 (500 ng/ml) for 30 minutes, after which surface expression of Cxcr4 was compared by flow cytometry. Gray/Black: Unstimulated; Red: Stimulated with SDF-1. Estimated MFI values are shown in the corresponding colors. Percent reduction of Cxcr4 expression was calculated as described (Materials and Methods section). Shown are representative data from three independent experiments. Mean values are indicated as bars ($n = 3$, *, $p < .05$; **, $p < .01$). **(C):** Transwell migration assay. Test HS(P)Cs (3×10^4 cells) were added to individual upper chambers of transwell plates in which lower chambers contained SDF-1 (50 ng/ml) as an attractant. After incubation for 90 minutes at 37°C, migrated cells were counted. Shown are representative data from two independent experiments with five replicates per group. ***, $p < .001$. The differences between groups were tested by Tukey-Kramer multiple comparison. Abbreviations: ΔC, C-terminal deletion; MFI, mean fluorescence intensity; SDF-1, stromal cell-derived factor 1; WT, wild type.

demonstrated overexpression of Cxcr4 receptors, either in wild-type configuration or in their C-terminus truncated form, in transduced HS(P)Cs (Fig. 1A; Supporting Information Fig. S4A, S4B) and in the murine hematopoietic cell line 32D (Supporting Information Fig. S4C). Defective internalization of ΔC-Cxcr4 in response to SDF-1/CXCL12, a feature predictable

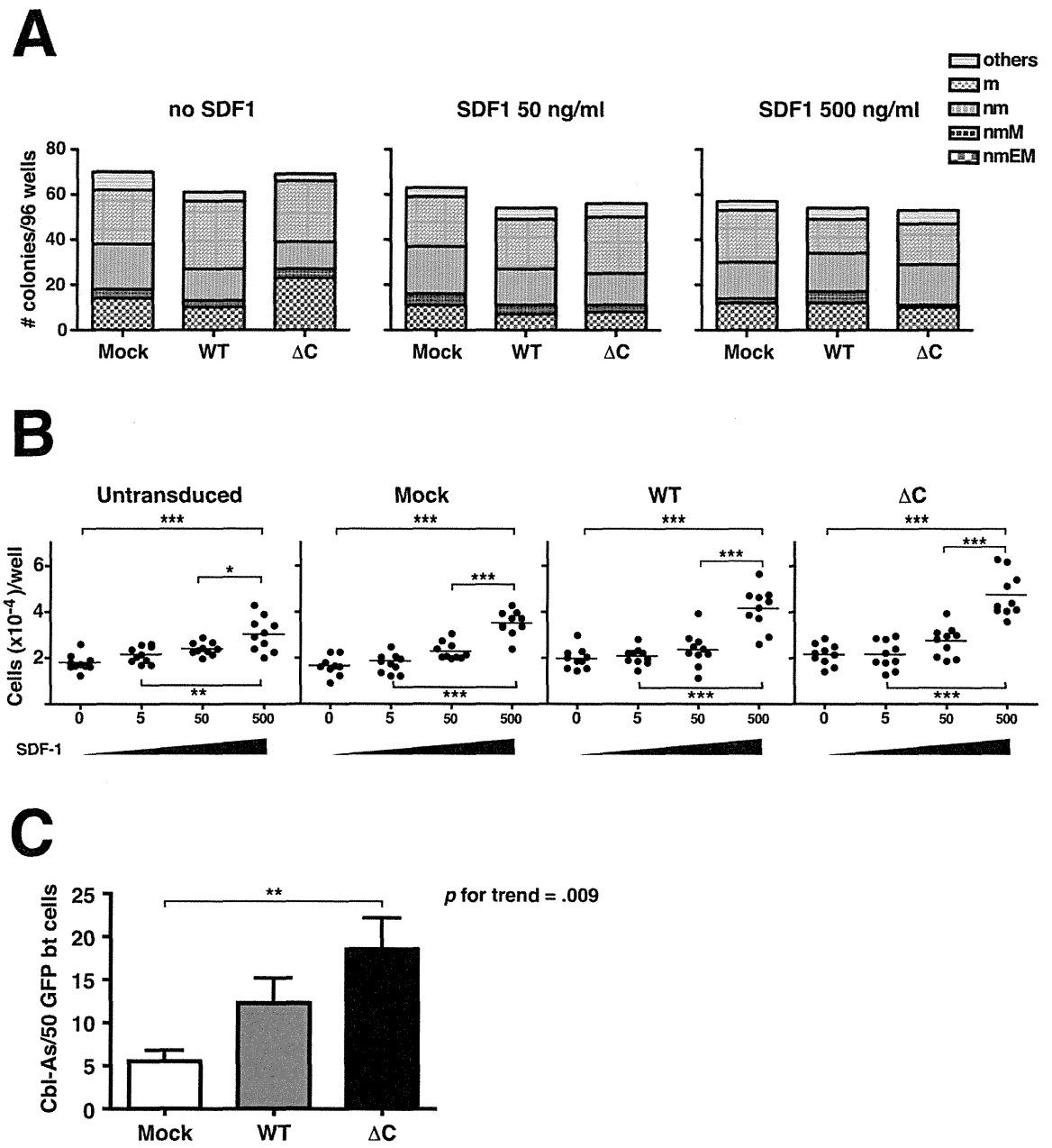

Figure 2. Augmentation of C-X-C chemokine receptor type 4 (Cxcr4) signaling in hematopoietic stem/progenitor cells (HS(P)Cs) correlates with enhanced proliferative responses in the presence of SDF-1 in high concentrations and of feeder cell layers. **(A):** Single-cell cultures in the presence of SCF, TPO, IL-3, and EPO as baseline cocktail. Cultures were maintained either with no other additives (no SDF-1) or added exogenous SDF-1 at the indicated concentrations (SDF-1 50 or 500 ng/ml). Shown are colony numbers (numbers of positive wells in a 96-well plate) and the colony types assessed on day 11. Cell composition morphologically determined in each colony was represented by a single or combination of the following letters; m: macrophage, n: neutrophil, E: Erythroblast, M: Megakaryocyte. For example, "m" means a colony containing only macrophages, whereas "nm" and "nmM" represent colonies composed of a mixture of corresponding cell lineages. "nmEM" represents colonies derived from "uncommitted"single cells with high potential for multilineage differentiation within a myeloid compartment. **(B):** Proliferation ability of *Cxcr4*-modified cells in response to SDF-1. Test HS(P)Cs were sorted at 50 cells per well into 96-well plates and were counted 7 days after cultivation in serum-free basal medium (containing SCF and TPO) alone or in the presence of SDF-1. Data shown represent three independent experiments ($n = 10$). Mean values are indicated as bars. *, $p < .05$; **, $p < .01$; ***, $p < .001$. Untransduced: Untransduced control. **(C):** Ability of *Cxcr4*-modified HS(P)Cs to form Cbl-As in the presence of feeder cells. Test cells were directly sorted onto a feeder layer of C3HT101/2 cells at 50 cells per well. Numbers of areas per well evaluated on day 10 are shown as mean values ± SD ($n = 4$, representative of three independent experiments). **, $p < .01$. Abbreviations: Cbl-As, cobblestone-like areas; GFP, green fluorescent protein; SDF-1, stromal cell-derived factor 1; WT, wild type.

from previous observations [14, 16–18, 39, 40], was clearly observed in transduced 32D cells with 100 ng/ml of SDF-1 (Supporting Information Fig. S5A). With this low concentration of SDF-1, however, as the degree of receptor internalization in both Mock- and WT-Cxcr4-transduced cells was far less in HS(P)Cs than that observed in other cells, including the

human T cell line CEM (Supporting Information Fig. S5C), blunting of the response of ΔC-Cxcr4 was therefore not evident (Supporting Information Fig. S5B). Nevertheless, HS(P)Cs overexpressing ΔC-Cxcr4 showed a blurred response in receptor internalization with a higher concentration of SDF-1 (500 ng/ml, Fig. 1B). Gain-of-function effects were confirmed in WT- and ΔC-Cxcr4-transduced cells in comparison with Mock-cells; a stepwise enhancement in transwell migration to SDF-1/CXCL12 was evident with greater response for ΔC-Cxcr4-cells (Fig. 1C; Supporting Information Fig. S6), consistent with an enhanced chemotactic response in human cells expressing WHIM-type CXCR4 [17, 18, 30, 41–43]. The stepwise nature of gain-of-function for WT- and ΔC-Cxcr4 was further confirmed with a Ca^{2+} influx assay using 32D cells (Supporting Information Fig. S7).

Enhanced In Vitro Proliferative Response of HS(P)Cs Under Particular Circumstances by Gain-of-Function Modification in Cxcr4 Signaling

We next examined the characteristics of these cultured HS(P)Cs using a series of in vitro assays. At first, clonogenic ability and differentiation characteristics were compared in in vitro single-cell liquid culture. As shown in Figure 2A, modification of Cxcr4 did not alter frequencies of HS(P)Cs capable of colony formation, with colony types also unaffected (no SDF-1). Addition of SDF-1 produced no remarkable influence on these cultures (SDF-1 50 and 500 ng/ml). These results suggest minimal influences of Cxcr4 receptor modification on HS(P)Cs' clonogenic ability in stroma-free liquid culture and on their differentiation properties. We next tested proliferative characteristics of bulk populations in liquid culture. As described (Supporting Information), our basal culture system is distinct from others in allowing self-renewal of murine HSCs both at a single cell level [24, 44] and at a population level [45] with the minimum cytokines (SCF and TPO) needed in a serum-free setting. In this so-called "HSC-self-renewal compatible" culture, we found fresh HSCs highly resistant to desensitization to Sdf-1 (Supporting Information Fig. S8). When cultured HS(P)Cs were tested in this system (input cells = 50 cells per well), massive expansion was observed for all cell types in the absence of SDF-1/CXCL12 (Fig. 2B, SDF-1: 0 ng/ml). Cell proliferation was unexpectedly enhanced in the presence of SDF-1/CXCL12 especially at the highest concentration (500 ng/ml), which was considered "desensitizing" for most cell types [16, 46, 47]. Interestingly, the additive effects of exogenous Cxcr4 receptors on HS(P)C proliferation became evident only in the presence of 500 ng/ml SDF-1; as shown in Supporting Information Figure S9, stepwise (i.e., WT < ΔC-Cxcr4) enhancement in response was observed in comparison with control samples (Untransduced and Mock).

We then tested whether overexpression of exogenous Cxcr4 affected HSPCs' ability to colonize and to repopulate C3H10T1/2 feeder cell layers in an in vitro coculture assay [33]. In this assay, test cells can be scored for in vitro clonogenic ability in the presence of stromal cells by counting characteristic cobblestone-like areas that form underneath the feeder layers. We first confirmed both the presence of Sdf-1 in this culture supernatant and the significance of the Sdf-1/Cxcr4 axis for cobblestone-like area formation using the CXCR4 antagonist AMD3100 (Supporting Information Fig. S10). When Cxcr4-modified HS(P)Cs were subjected to this assay, the ability to form cobblestone-like areas proved remarkably enhanced in comparison with that in Mock control cells; enhancement occurred in a stepwise manner, with the greatest response in ΔC-Cxcr4-overexpressing cells (Fig. 2C). Collectively, these findings demonstrated that augmented Cxcr4 signaling alters cellular responses to favor HSPC survival/proliferation, especially in the presence of high concentrations of Sdf-1 and/or of supporting feeder layers that produce this ligand.

Augmented Cxcr4 Signaling in Murine HS(P)Cs/HSPCs Does not Enhance BM Homing/Lodging but Improves Subsequent BM Repopulation

We then examined how augmentation in Cxcr4 signaling affected the in vivo behavior of transplanted HS(P)Cs at different times during BM reconstitution. As the earliest process, BM homing efficiency was assessed using $EGFP^+$ cultured HSPC populations (Supporting Information Figs. S1B, S2A). As shown, we found no enhancement in BM homing of HSPCs at the indicated times (4–24 hours) by gain-of-function Cxcr4 modification (Fig. 3A; Supporting Information Fig. S2B). This was also true when we used $EGFP^+$ cultured HS(P)Cs as the sole transplants and assessed BM homing by counting number of CFCs recovered from each recipient at 16 and 24 hours (Fig. 3B). We next examined subsequent BM repopulation kinetics by extending the times of analysis, similarly as previously reported [33]: in this setting, CFCs measurable in BM are supposed to reflect not only homing but also subsequent cell division shortly after homing. As shown in Figure 3C, augmentation of Cxcr4 signaling in HS(P)Cs did not lead to increased numbers of CFCs in recipient BM at days 2 and 4. Collectively, these results demonstrate that augmentation in murine Cxcr4 signaling does not affect the earliest events after HSPC transplantation, including BM homing/lodging by HSPCs.

We further tracked in vivo BM repopulation by donor HS(P)Cs beyond the above time points. As recipients of HS(P)Cs alone barely survived lethal-dose irradiation beyond day 7, test HS(P)Cs were transplanted with competitor cells, with their relative contributions to BM repopulation determined at days 14 and 21 (Fig. 3D). Of note is that stepwise increases in donor chimerism were visible in BM at these time points (p for trend = .038) with ΔC-Cxcr4-cells showing the highest donor cell contribution (*vs.* Mock, $p = 0.035$).

The advantage in BM repopulation for Cxcr4-augmented HS(P)Cs was also noticeable in cohorts of long-term recipients (Fig. 3E, p for trend = .042), again with ΔC effects being the highest (vs. Mock, $p = .038$). From these observations, we conclude that the Sdf-1/Cxcr4 axis plays a role in productive BM repopulation by transplanted HSPCs after the second phase (weeks 2–3) that follows transplantation.

Continuous Overexpression of Exogenous Cxcr4 Receptors in HS(P)Cs Leads to Poor Peripheral Reconstitution

The possible correlation between Cxcr4 signal intensity in HS(P)Cs and their short-term BM reconstitution efficiency made us wonder how long-term transplantation outcome would fare in gain-of-function experiments. In competitive repopulation assays, ΔC-Cxcr4-transduced HS(P)Cs contributed poorly to PB chimerism at 4 weeks (data not shown) and 16

weeks (Fig. 4A), consistent with the major features of WHIM syndrome, lymphocytopenia and neutropenia [15, 16, 19, 41, 48]. That overexpression of WT-Cxcr4 in HS(P)Cs also did not improve PB reconstitution (Fig. 4A, WT) was unexpected, as beneficial effects of similar treatment are reported for human $CD34^+$ cells [13, 14]. Systemic injection of the Cxcr4 antagonist AMD3100 into long-term recipients increased PB donor chimerism significantly in WT- and ΔC-Cxcr4 groups, suggesting that blunted peripheral mobilization of donor cells played a causal role in poor PB reconstitution in these mice (Fig. 4B; Supporting Information Fig. S11).

Enhanced Donor Cell Chimerism Occurs in BM Cells Throughout Developmental Stages of HS(P)Cs Expressing Gain-of-Function Cxcr4 Receptors

Of note is that the recipients of ΔC-Cxcr4-transduced HS(P)Cs showed obvious long-term donor cell chimerism in BM (Fig. 3E); this may accompany favorable in vivo expansion of

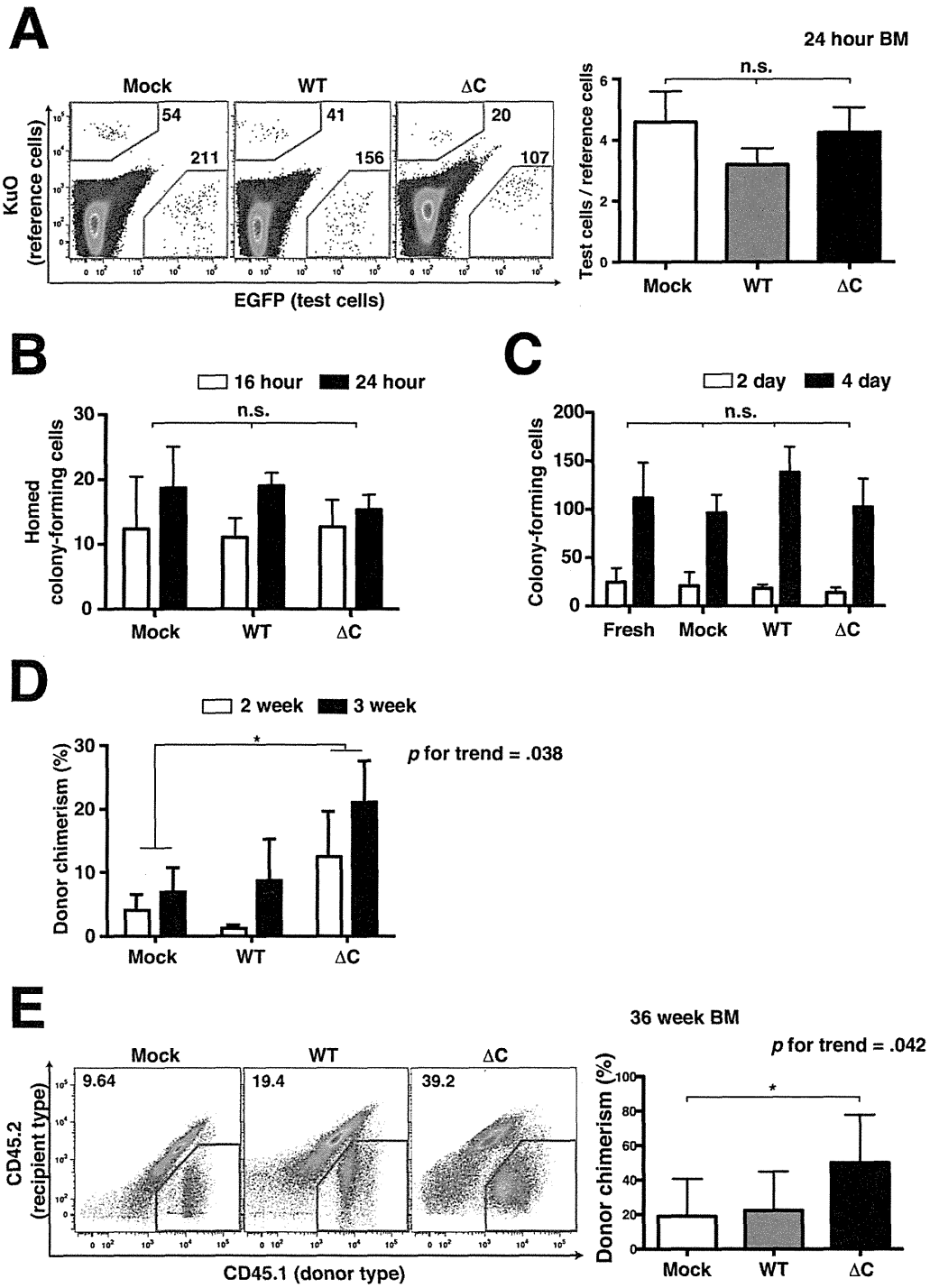

transplanted HSCs or may simply indicate accumulation of certain cell types at a particular differentiation stage, thus reflecting conditions that in some respect are abnormal. To distinguish these possibilities, we scrutinized recipient BM for donor cell chimerism in multiple cell compartments, including the long-term HSC fraction (LT-HSC; Supporting Information Fig. S12). As shown in Figure 4C, individual recipients of Mock-treated HS(P)Cs did not display significant alterations in donor cell chimerism among these populations, suggesting little influence on hematopoiesis by Mock transduction of HS(P)Cs. In contrast, donor cell chimerism differed clearly between PB leukocytes (open histograms) and BM compartments (colored histograms) in each recipient that received Cxcr4 signal-enhanced HS(P)Cs (Fig. 4C, WT and ΔC). General enhancement of chimerism in the BM compartments, including LT-HSC, was striking, with no difference between fractions, which suggested that Cxcr4 signal-dependent donor cell expansion might occur even at a stem cell level. When donor cell chimerism was similarly assessed along two major paths of lineage development, that is, B cells and neutrophils, results were consistent with the idea that Cxcr4 signal augmentation induced no gross alterations, such as maturation arrest, in hematopoietic development, but likely caused exaggerated BM retention of donor cells (Fig. 4C). The increase of "phenotypically-defined" LT-HSCs might not necessarily imply, however, that functional HSC numbers were amplified. We could demonstrate persistence within primary recipient BM of reconstituting cells that were capable of establishing donor chimerism upon serial transplantation (Supporting Information Fig. S13, PB). No advantage over Mock-treated cells, however, was observed for WT- and ΔC-Cxcr4-expressing cells in repopulation of secondary recipient BM (Supporting Information Fig. S13, BM), unlike the case with primary recipients (Fig. 3E) (see Discussion section).

Loss-of-Function Studies Support the Proposed Roles of Cxcr4 in Murine HSPCs in Transplantation

To understand Cxcr4's roles in murine HSPCs better in transplantation, we conducted loss-of-function analyses in experimental settings like those used for the gain-of-function studies. To this end, we mostly used purified HSCs obtained from *Cxcr4* conditional KO mice [49] and littermate (LM) control mice after induction (Supporting Information). First, the absence of Cxcr4 receptors did not affect HSCs' colony-forming ability in liquid medium or their multilineage potentials (Fig. 5A). When cell proliferation was tested in liquid culture, we found loss of SDF-1-responsiveness in KO-HSCs (Fig. 5B, KO) whereas control LM-HSCs showed a response similar to that observed in both fresh B6 HSCs (Supporting Information Figs. S8, S15A) and cultured HS(P)Cs (Fig. 2B). Consistent with the loss of SDF-1-response phenotypes, the ability of Cxcr4-deficient HSCs to form cobblestone-like areas was shown to be severely impaired (Fig. 5C). The defect in Cxcr4-KO-HSCs found in this assay may be regarded as a mirror image of the results in gain-of-function experiments (Fig. 2C), thus further supporting the importance of Cxcr4 receptors in HSC/HSPC colonization and proliferation in the presence of feeder cell environments that produce Sdf-1/Cxcl12.

We then examined how the absence of Cxcr4 signaling in HSCs affected in vivo kinetics of donor cell repopulation. Early BM homing was assessed using fresh HSPCs with or without receptor desensitization using the Cxcr4 antagonist AMD3100 following established preincubation methods [37–39]. As assessed at 15 hours, we did not detect a decrease in BM homing of HSPCs that had been rendered unresponsive to Sdf-1/Cxcl12, even with additional systemic administration of AMD3100 (Fig. 5D; Supporting Information Fig. S3). Supporting this observation, assessment of subsequent repopulation in BM on days 4 and 6 demonstrated that in the absence of Cxcr4 expression (KO), transplanted HSCs yielded numbers of CFCs comparable with those observed for wild type HSCs (LM; Fig. 5E). Genotyping polymerase chain reaction demonstrated that most randomly picked-up CFCs had the Cxcr4 locus completely knocked out (31 in 33, 93.9%), thus indicating that the "highly purified HSCs" that we injected alone into lethally irradiated recipients were capable of BM homing in vivo and colony formation ex vivo in the absence of functional Cxcr4 expression. KO-HSCs, contrary to these findings, clearly showed significant impairment in capability of BM repopulation at 2 and 3 weeks after transplantation (Fig. 5F). As expected, KO-HSCs contributed to PB long-term less than did LM control HSCs (Fig. 5G), consistent with previous observations [7, 8, 12].

Our comprehensive approach has pointed out the importance of the Sdf-1/Cxcr4 axis in HSC/HSPCs for productive

Figure 3. Augmentation of C-X-C chemokine receptor type 4 (Cxcr4) signaling does not affect early homing/lodging processes but likely enhances subsequent BM repopulation by murine hematopoietic stem/progenitor cells (HS(P)Cs). Tracking in vivo fates within recipient BM of reconstituting HS(P)Cs with or without overexpression of gain-of-function Cxcr4 receptors. **(A):** Homing assay using cultured HSPCs, either Mock-virus-treated (Mock) or expressing either WT or C-terminal truncated-type (ΔC) exogenous Cxcr4 receptors. These test cells (50,000 cells, $EGFP^+$) and fresh c-$Kit^+Sca\text{-}1^+$Lineage marker-negative cells expressing KuO protein (17,000 cells) were intravenously infused into lethally irradiated recipient mice. Twenty-four hours later, homing events were quantified in recipient BM as KuO^+ and $EGFP^+$ cells (red and green gates, respectively). Representative flow cytometry analysis is shown at left. Shown are the event ratios of $EGFP^+$ (test cells) to KuO^+ (reference cells) expressed as means ± SD ($n = 5$ for each group). **(B, C):** Assessment of BM homing/early repopulation processes. Shown are numbers of colony-forming cells detected in BM of each mouse that received either fresh unmodified HSCs or HS(P)Cs (200 cells per mouse) alone after lethal-dose irradiation. Shown are the results obtained at 16 hours (open histograms) and 24 hours (closed histograms) after transplantation **(B)**, or at 2 days (open histograms) and 4 days (closed histograms) after transplantation **(C)**. Data are expressed as means ± SD ($n = 4$, representative of three independent experiments). **(D):** Donor cell chimerism assessment in competitive repopulation assays. Shown are donor cell chimerism values in recipient BM at week 2 (open histograms) and week 3 (closed histograms). Mean values ± SD are shown ($n = 4$, representative of four independent experiments). *, $p < .05$ (ΔC vs. Mock). Values of p for trend are shown. **(E):** Donor cell chimerism in long-term recipient BM at week 36. Shown is representative flow cytometry analysis of donor cell chimerism in mice transplanted with treated HS(P)Cs in a competitive repopulation assay. Graphic representation of chimerism analysis is also shown as mean values ± SD ($n = 5$, representative of three independent experiments). *, $p < .05$ (ΔC vs. Mock). Values of p for trend are shown. Abbreviations: BM, bone marrow; ΔC, C-terminal deletion; EGFP, enhanced green fluorescent protein; KuO, Kusabira Orange; WT, wild type.

engraftment and repopulation in recipient BM, especially for a particular phase after transplantation, that is, the early/sub-early repopulation phase (~2–3 weeks), which follows the initial engraftment process (<1 week).

Alteration in Phosphorylation Kinetics of Erk in Response to SDF-1 in HS(P)Cs Expressing ΔC-Cxcr4

To obtain mechanistic insights, we examined how overexpression of exogenous Cxcr4 receptors altered downstream

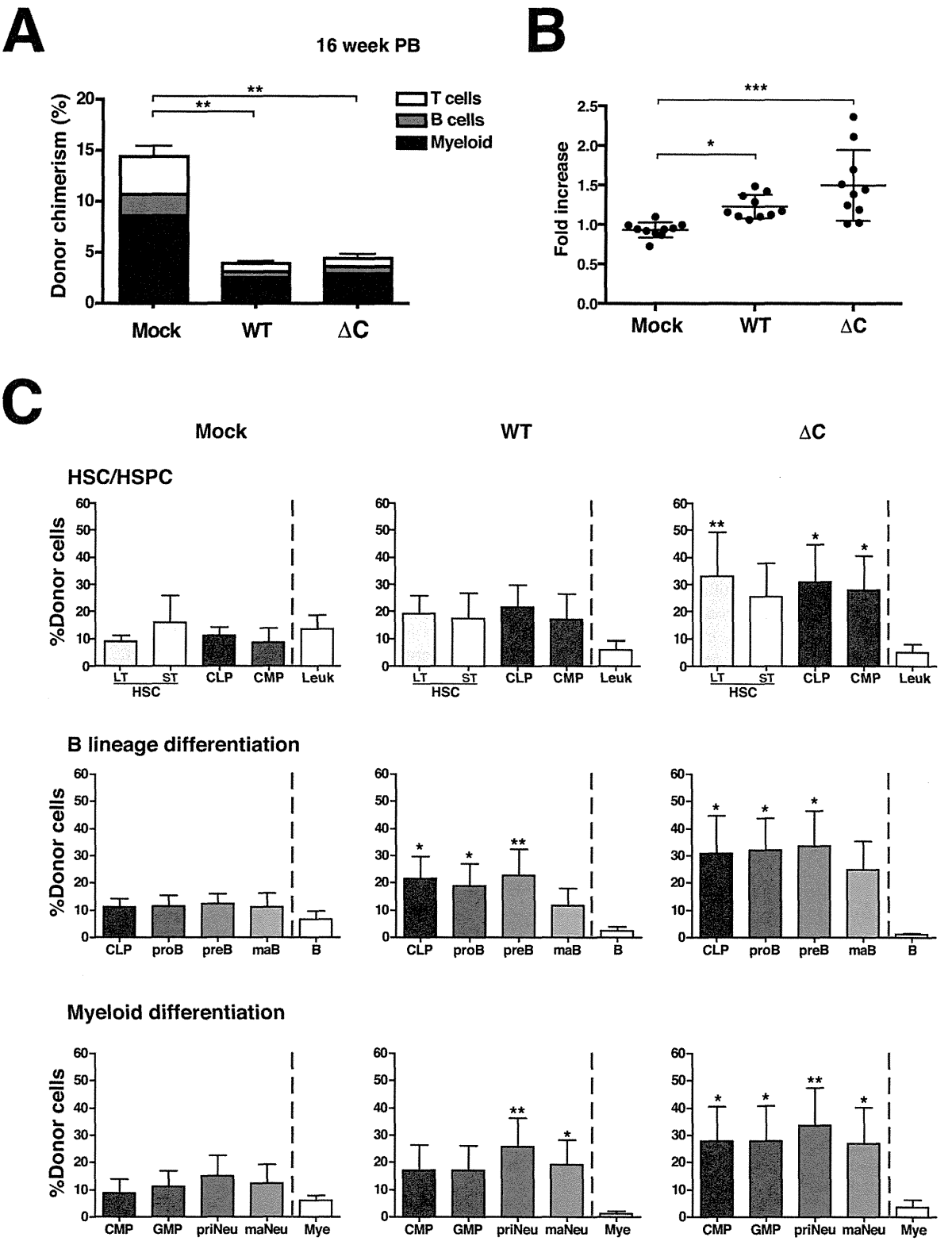

signaling events in HS(P)Cs. Phosphorylation kinetics in Erk1/2 and Akt were tested in $EGFP^+$ cultured HS(P)Cs by flow cytometry analysis. While phosphorylated Akt intensity was unaltered before and after stimulation (Supporting Information Fig. S15), clear alterations in phosphorylated Erk1/2 (pErk) signals confirmed that the HS(P)Cs used the MAPK/Erk signaling pathway in response to SDF-1/CXCL12 (Fig. 6). The peak response was seen 3 minutes after stimulation, with the greatest response in ΔC-Cxcr4-expressing cells. Response termination was delayed in ΔC-Cxcr4-expressing cells, with residual pErk-signals still detectable at 15–30 minutes, whereas cells in the other two samples (Mock and WT) quickly returned to baseline status by 15 minutes. Of note is that with even a "desensitizing-high" concentration of SDF-1 (500 ng/ml), ΔC-expressing cells still showed visibly enhanced phosphorylation at peak and delay in its termination. Similar behavior was confirmed using the 32D murine hematopoietic cell line (Supporting Information Fig. S4D).

Discussion

Our goal is to use experimental findings to benefit patients undergoing transplantation. To this end, we sought to clarify the stage-specific role of Cxcr4 signaling in transplanted cells during hematopoietic reconstitution. With gain-of-function experiments, augmentation of Cxcr4 signaling appeared relatively unimportant in accelerating the homing/lodging of murine HSC/HSPCs but efficient in enhancing their subsequent repopulation of BM. This pattern of stage-specificity in Cxcr4's role was also demonstrated in a series of loss-of-function experiments. Our results strengthen the generally held idea that CXCR4 signal modification can benefit transplantation outcomes [13, 14], by demonstrating enhancement in donor cell expansion, possibly even at a stem cell level. Also to note, however, is that sustainment of augmented signal led to detrimental effects on transplantation outcomes in this study, even with overexpression of a non-mutant Cxcr4 receptor.

That the SDF-1/CXCR4 axis plays an indispensable role in BM homing by adult HSCs seems widely accepted [50, 51]; this may contrast with our findings. This view, however, rests on pioneering studies that used human HSPCs, mostly in loss-of-function settings [12, 52]. These were followed by gain-of-function studies that demonstrated improved human HSPC engraftment in immunodeficient mice with overexpression of wild-type CXCR4 [13, 14, 19]. KO mouse studies have clearly demonstrated the importance of Cxcr4 for robust hematopoietic reconstitution in transplantation but have not specifically addressed BM homing by purified HSCs [7, 8]. Our study of the role of Cxcr4 is, so far as we know, the first gain-of-function approach to use murine HSC/HSPCs. Using cultured HSPCs derived from KSL cells, we demonstrated that overexpression of exogenous Cxcr4 receptors did not lead to enhanced BM homing (Fig. 3A; Supporting Information Fig. S2). Short-term homing (16–24 hours) and subsequent repopulation kinetics (days 2–4) in BM, assessed by using cultured HS(P)Cs, also did not alter with Cxcr4 overexpression (Fig. 3B, 3C). These results indicate that augmentation of Cxcr4 signaling does not benefit transplanted murine HSC/HSPCs in these early processes.

In loss-of-function experiments, we used purified HSCs freshly isolated from Cxcr4-deficient mice for the assessment of early BM repopulation capability (days 4 and 6; Fig. 5E). The results supported the idea that the Sdf-1/Cxcr4 axis may be of little importance in this phase of BM repopulation. The impact of Cxcr4 signaling on early BM homing was assessed using fresh, uncultured HSPCs following established desensitizing methods using the Cxcr4 antagonist AMD3100 [37–39]. Our results demonstrated that BM homing (15 hours) of purified HSPCs did not much depend on the Sdf-1/Cxcr4 axis, consistent with previous observations [37]. There may be controversy, however, on this issue, because other workers observed impaired BM homing by HSPCs after AMD3100 treatment [38, 39]. This can probably be attributed to differences in study design, with the most significant one being that we used HSPCs alone as the sole transplant/analyte whereas others assessed homing of HSPCs by injecting donor cells preincubated with AMD3100 as either low-density BM cells [38] or lineage-negative BM cells [39]. We emphasize the importance of these observations, as in clinical settings unpurified hematopoietic cells are most often used in transplantation. Nevertheless, we believe that our findings also are of importance, because clinical gene therapy trials currently in progress use purified $CD34^+$ HSPCs [53], thus resembling our experimental settings.

Figure 4. Continuous expression of gain-of-function receptors in HS(P)Cs leads to impaired peripheral reconstitution, but enhanced bone marrow (BM) repopulation, by donor cells throughout developmental stages. **(A):** Percent PB chimerism of donor cells on competitive repopulation assay 16 weeks after transplantation. Donor cell chimerism was separately determined for each lineage (T cells, B cells, and myeloid cells). Shown are data represented as mean values ± SD obtained from mice each of which received 700 enhanced green fluorescent protein positive cells along with 2×10^5 competitor cells ($n = 5$, representative of three independent experiments). **, $p < .01$. **(B):** Assessment of AMD3100-induced mobilization effect on donor chimerism in long-term recipients. One week after the analysis of baseline donor cell chimerism, each mouse received intraperitoneal systemic injection of AMD3100 (10 mg/kg). One hour after AMD3100 injection, PB chimerism was analyzed and the fold increase of donor chimerism was calculated for each donor. Shown are data represented as mean values ± SD obtained from groups of recipient mice ($n = 10$, representative of two independent experiments). *, $p < .05$; ***, $p < .001$. Individual data are shown in Supporting Information Fig. S11. **(C):** Donor cell chimerism assessed 36 weeks after transplantation in long-term recipient BM (colored histograms) and PB (white histograms) for multiple hematopoietic subfractions. Top: Stem cells, progenitor cells, and PB leucocytes (HSC/HSPC). Middle: Differentiation path along B cell development (B lineage differentiation). Bottom: Differentiation path along myeloid development (myeloid differentiation). Detailed marker combinations used to define each population are listed (Supporting Information Materials). Data analyzed by Dunnett's multiple comparison test with peripheral chimerism as control. *, $p < .05$; **, $p < .01$. Abbreviations: B, B cells in PB; ΔC, C-terminal deletion; CLP, common lymphoid progenitors; CMP, common myeloid progenitors, all in BM; GMP, granulocyte/macrophage progenitors; HSPC, hematopoietic stem/progenitor cell; Leuk: leukocytes in PB; LT-HSC, long-term hematopoietic stem cells; maB, mature B cells; maNeu, mature neutrophils, all in BM; Mye, myeloid cells in PB; PB, peripheral blood; proB, pro-B cells; preB, pre-B cells; all in BM; priNeu: primitive neutrophils; ST-HSC, short-term hematopoietic stem cells; WT, wild type.

In contrast to the above findings, studies of donor cell reconstitution within BM at weeks 2 and 3 clearly accorded a role to Cxcr4 signaling (Figs. 3D, 5F). Although the frequency of donor HSCs in BM could not be determined by immunophenotyping at these early time points, the results obtained by cobblestone-like area formation experiments (Fig. 2C) mirrored in vivo donor chimerism at 2–3 weeks (Fig. 3D). This in turn supports the idea that augmentation of Cxcr4 signaling leads to expansion (colonization, proliferation) of HSPCs in vivo, where the presence of stromal cells is expected to promote this event.

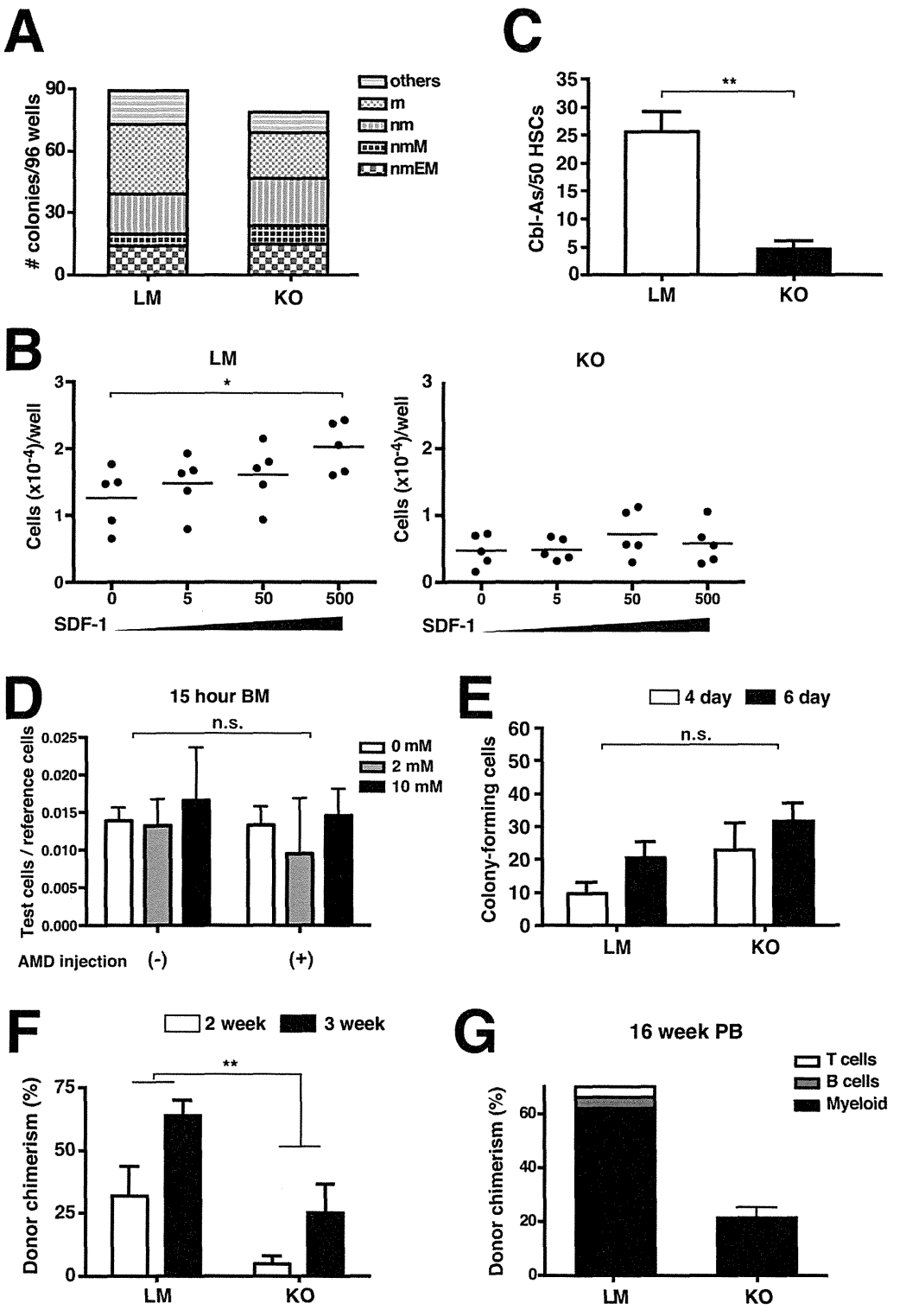

Cxcr4-mediated effects on in vivo HSC/HSPC expansion may arise from improved survival/proliferation and/or enhanced retention of HSPCs within BM. Consistent with this idea, studies suggested that CXCR4 relays a survival-promoting signal within HSPCs [51, 54]. Of note is that Cxcr4 signal-mediated enhancement in proliferation was more evident when HSPCs either were in contact with feeder cells (Fig. 2C) or were stimulated with SDF-1 in high concentrations (500 ng/ml, Fig. 2B; Supporting Information Fig. S9). Promotion of cell cycling in HSPCs by SDF-1/CXCL12 may conflict with recent descriptions of a role for Cxcr4 in maintenance of HSC quiescence [7, 8, 11]. We, however, think it possible to explain this discrepancy by the difference in culture systems. In fact, in our defined culture system HSCs, either fresh or after stimulation, resisted desensitization to high concentrations of SDF-1 (Figs. 2B, 5B; Supporting Information Fig. S8) [44, 45]. As we could readily detect measurable levels of Sdf-1 in murine BM cavities irrespective of irradiation conditioning (Supporting Information Fig. S10B), one can expect local levels of Sdf-1 to be very high in vivo, especially in the functional niche environment. We therefore speculate that in our scenario, high concentrations of Sdf-1 may favor proliferative response in murine HSC/HSPCs when they exist in "self-renewal-compatible" conditions. Altered Erk activation kinetics may be responsible for the observed enhancement of repopulation capability in HSC/HSPCs equipped with gain-of-function Cxcr4, but further investigation is needed for more mechanistic insights.

When considering implications of our study for clinical transplantation, poor PB contribution by HS(P)Cs overexpressing WT-Cxcr4 is significant; this may contrast with the favorable effects of CXCR4 overexpression on the engraftment/repopulation of human HSPCs [13, 14]. Species differences may account for this discrepancy. Differences in study design, however, may contribute more importantly. We transplanted only cells expressing EGFP at high levels (thus likely exogenous Cxcr4 receptors as well, see Supporting Information Fig. S4A), which might have led to unfavorable, extreme gain-of-function effects on hematopoietic reconstitution. Alternatively, improved reconstitution reported in the case of CXCR4 overexpression may be attributable to the coinjection of non-HSC/HSPCs, so-called "facilitating cells" [50], mostly missing in our study.

We must note that as our work required the cultivation of HSCs in gain-of-function settings, thus our findings may be applicable to cycling HSC/HPSCs (likely present in the setting of gene therapy) but not to their fresh counterparts. Our culture system, however, is capable of maintenance of progenitor phenotypes in most cells after 7 days (Supporting Information Fig. S14B, S14C) and actually is "self-renewal compatible" [44, 45]. We therefore believe that this study complements general knowledge concerning the role of CXCR4 in HSPC transplantation [51, 55, 56].

Kawai et al. [19] demonstrated that transplantation of human HSPCs overexpressing WHIM-mutant receptor resulted in the WHIM phenotype in the mouse environment. More recently, generation of WHIM-type mice was reported with many interesting findings [16]. Ours is the first study of the WHIM-type receptor in the murine system in the context of HSPC transplantation. Most notable is that enhanced BM repopulation was observed in the LT-HSC population, at least as defined by immunophenotyping, upon signal augmentation (Fig. 4C). Secondary transplantation, however, did not confirm stem cell expansion in primary BM by definition (Supporting Information Fig. S13, PB); this was partly explained by the properties of "defects in PB release," which should inhere in phenotypically defined HSCs still expressing exogenous Cxcr4. Furthermore, the highest donor chimerism by ΔC-Cxcr4-expressing cells in BM (Fig. 3E) was not phenocopied to the BM of secondary recipients (Supporting Information Fig. S13, BM), probably suggesting impaired repopulating ability in each donor LT-HSC due to long-term nonphysiological Cxcr4 signaling events. Further investigation is necessary for formal demonstration of whether enhanced HSC self-renewal is

Figure 5. Loss-of-function studies support the importance of the Sdf-1/Cxcr4 axis in HSC/hematopoietic stem/precursor cell (HSPCs) for BM repopulation in the early/sub-early phase after transplantation. All loss-of-function studies (except those illustrated in (D)) used as starting materials purified HSCs harvested from either *Cxcr4* conditional KO mice or their LM control mice similarly treated with pIpC. **(A):** Single-cell cultures in the presence of SCF, TPO, IL-3, and EPO. Shown are colony numbers and the colony types assessed on day 14. m: macrophage, n: neutrophil, E: Erythroblast, M: Megakaryocyte (classifications, m, nm, nmM, and nmEM). **(B):** Proliferation ability of either LM HSCs or *Cxcr4*-KO HSCs in response to SDF-1 (starting from 50 cells per well). Data shown represent three independent experiments ($n = 5$). Mean values are indicated as bars. *, $p < .05$. **(C):** Ability of either LM HSCs or *Cxcr4*-KO HSCs to form Cbl-As in a feeder layer of C3H10T1/2 cells (50 input cells per well). Shown are numbers of areas per well evaluated on day 10 as mean values ± SD ($n = 4$, representative of three independent experiments). **, $p < .01$. **(D–F):** Tracking in vivo fates of reconstituting HSC/HSPCs in the initial (**D**, < 24 hours) and early/sub-early (**E**, days 4–6; F, weeks 2–3) phases within BM. **(D):** BM homing assay using fresh HSPCs. Test cells were from Kusabira Orange transgenic (KuO-Tg) mice (10,000 KuO^+ c-Kit^+Sca-1^+Lineage marker-negative (KSL) cells). Fresh BM cells from EGFP-Tg mice were used as reference cells (10^6 cells). Test cells either were left untreated or were incubated with AMD3100 for 30 minutes at 37°C at the indicated concentration before transplantation. Lethally irradiated recipients received a mixture of test and reference cells. Fifteen hours later, homing events were quantified in recipient BM as KuO^+ and $EGFP^+$ cells. One group of mice received PBS intraperitoneally [AMD injection (−)], whereas another received AMD3100 [AMD injection (+)]. Shown are the event ratios of test cells (KuO^+) to reference cells (enhanced green fluorescent protein positive) as means ± SD (n = 4 for each group). **(E):** Shown are numbers of colony forming cells detected in BM of each mouse that received either LM HSCs or KO HSCs (100 cells per mouse) at day 4 (open histograms) and day 6 (closed histograms). Data are expressed as means ± SD ($n = 5$, representative of two independent experiments). **(F):** Donor cell chimerism in recipient BM at week 2 (open histograms) and week 3 (closed histograms) is shown as mean values ± SD ($n = 5$, representative of three independent experiments). **, $p < .01$. **(G):** Percent PB chimerism of donor cells on competitive repopulation assay 16 weeks after transplantation. Donor cell chimerism was separately determined for each lineage (T cells, B cells, and myeloid cells). Shown are data represented as mean values ± SD obtained from mice each of which received 100 $CD34^-$KSL cells along with 2×10^5 competitor cells. Abbreviations: BM, bone marrow; Cbl-As, cobblestone-like areas; HSC, hematopoietic stem cell; KO, knock out; m, colony containing only macrophages; nm and nmM, colonies composed of a mixture of corresponding cell lineages; nmEM, colonies derived from "uncommitted"single cells with high potential for multilineage differentiation within a myeloid compartment; LM, litter mate; PB, peripheral blood; SDF-1, stromal cell-derived factor 1.

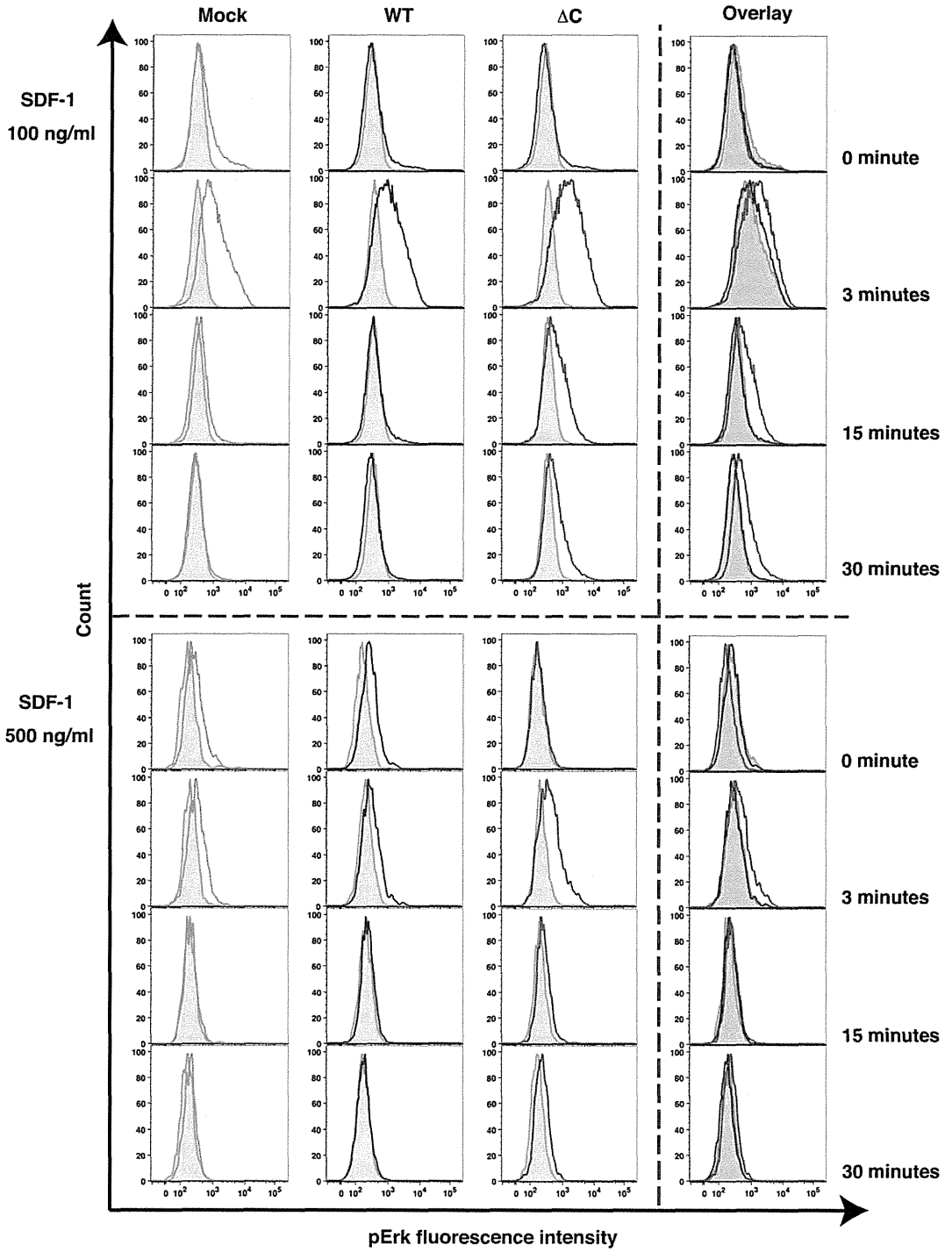

Figure 6. Augmentation of C-X-C chemokine receptor type 4 signaling leads to enhanced and prolonged phosphorylation of Erk in hematopoietic stem/progenitor cells upon SDF-1 stimulation. Altered Erk activation kinetics. Test cells were cytokine-starved and stimulated with 100 or 500 ng/ml SDF-1 for the indicated times. The amount of phosphorylated Erk was determined by flow cytometry analysis. Top, each colored histogram represents pErk intensity at different time points upon stimulation with 100 ng/ml SDF-1. Bottom, same as top panel except for SDF-1 concentration (500 ng/ml). Gray histogram in each represents isotype-control. Overlay histogram figures are shown on the right for comparison between groups. Abbreviations: pErk, phospho extracellular signal-regulated kinase; SDF-1, stromal cell-derived factor 1; WT, wild type.

feasible, using an experimental system that allows in vivo inducible expression of exogenous Cxcr4 in test cells for a certain period of time after transplantation. More practically, it would be intriguing, for clinical application of our findings, to aim at drug discovery by screening for an efficacious and specific small molecule having characteristics of a CXCR4 agonist with limited desensitization. With elucidation of mechanisms underlying CXCR4/Cxcr4 signal-mediated effects, perhaps combined multiple strategic approaches will eventually culminate in greater clinical benefits.

Conclusion

We have addressed stage-specific roles for Cxcr4 signaling in donor cell repopulation in BM for the first time using purified mouse HSC/HSPCs. With unique combinational approaches that used both loss-of-function and gain-of-function modification of Cxcr4 receptors, we found that Cxcr4 signaling appears unimportant for the homing/lodging of mouse HSC/HSPCs but vital for their subsequent repopulation of BM. Cxcr4 signal enhancement likely favored BM repopulation by donor cells at a level of primitive cell populations, but was shown to be detrimental to PB reconstitution when sustained too long. Consequently, we think it important to investigate further when and how long signaling via this chemokine receptor is to be modified in order to favorably enhance HSPC engraftment in future transplantation medicine.

Acknowledgments

We thank Dr. A.S. Knisely for critical reading of the manuscript, Y. Yamazaki, J. Ooehara, R. Yamamoto, and S. Iriguchi for their technical assistance, B.I. Choi for Cxcr4-conditional KO mice, S. Hamanaka for Kusabira Orange Tg mice, T. Ogaeri for his advice on the C3H10T1/2-cocluture assay, and Huan-Ting Lin for his critical comments. This work was supported by grants from the Ministry of Education, Culture, Sport, Science and Technology, Japan and the Ministry of Health, Labour and Welfare, Japan.

Author Contributions

C.-Y.L. and M.O.: conception and design, collection and/or assembly of data, data analysis and interpretation, and manuscript writing; S.Y., M.O., S.S., and S.K.: collection and/or assembly of data; Y.M., Y.I., M.O., and Y.I.: provision of study material or patients; M.N.: data analysis and interpretation; H.N.: financial support and manuscript writing.

Disclosure of Potential Conflicts of Interest

The authors indicate no potential conflict of interest.

References

1 Buckley RH. Transplantation of hematopoietic stem cells in human severe combined immunodeficiency: Longterm outcomes. Immunol Res 2011;49:25–43.

2 Copelan EA. Hematopoietic stem-cell transplantation. N Engl J Med 2006;354:1813–1826.

3 Jenq RR, van den Brink MR. Allogeneic haematopoietic stem cell transplantation: Individualized stem cell and immune therapy of cancer. Nat Rev Cancer 2010;10:213–221.

4 Cancelas JA, Jansen M, Williams DA. The role of chemokine activation of Rac GTPases in hematopoietic stem cell marrow homing, retention, and peripheral mobilization. Exp Hematol 2006;34:976–985.

5 Wilson A, Oser GM, Jaworski M et al. Dormant and self-renewing hematopoietic stem cells and their niches. Ann N Y Acad Sci 2007;1106:64–75.

6 Nagasawa T, Omatsu Y, Sugiyama T. Control of hematopoietic stem cells by the bone marrow stromal niche: The role of reticular cells. Trends Immunol 2011;32:315–320.

7 Nie Y, Han YC, Zou YR. CXCR4 is required for the quiescence of primitive hematopoietic cells. J Exp Med 2008;205:777–783.

8 Sugiyama T, Kohara H, Noda M et al. Maintenance of the hematopoietic stem cell pool by CXCL12-CXCR4 chemokine signaling in bone marrow stromal cell niches. Immunity 2006;25:977–988.

9 Wright DE, Bowman EP, Wagers AJ et al. Hematopoietic stem cells are uniquely selective in their migratory response to chemokines. J Exp Med 2002;195:1145–1154.

10 Kawabata K, Ujikawa M, Egawa T et al. A cell-autonomous requirement for CXCR4 in long-term lymphoid and myeloid reconstitution. Proc Natl Acad Sci USA 1999;96:5663–5667.

11 Tzeng YS, Li H, Kang YL et al. Loss of Cxcl12/Sdf-1 in adult mice decreases the quiescent state of hematopoietic stem/progenitor cells and alters the pattern of hematopoietic regeneration after myelosuppression. Blood 2011;117:429–439.

12 Peled A, Petit I, Kollet O et al. Dependence of human stem cell engraftment and repopulation of NOD/SCID mice on CXCR4. Science 1999;283:845–848.

13 Brenner S, Whiting-Theobald N, Kawai T et al. CXCR4-transgene expression significantly improves marrow engraftment of cultured hematopoietic stem cells. Stem Cells 2004;22:1128–1133.

14 Kahn J, Byk T, Jansson-Sjostrand L et al. Overexpression of CXCR4 on human CD34+ progenitors increases their proliferation, migration, and NOD/SCID repopulation. Blood 2004;103:2942–2949.

15 Hernandez PA, Gorlin RJ, Lukens JN et al. Mutations in the chemokine receptor gene CXCR4 are associated with WHIM syndrome, a combined immunodeficiency disease. Nat Genet 2003;34:70–74.

16 Balabanian K, Brotin E, Biajoux V et al. Proper desensitization of CXCR4 is required for lymphocyte development and peripheral compartmentalization in mice. Blood 2012;119:5722–5730.

17 Diaz GA, Gulino AV. WHIM syndrome: A defect in CXCR4 signaling. Curr Allergy Asthma Rep 2005;5:350–355.

18 McDermott DH, Lopez J, Deng F et al. AMD3100 is a potent antagonist at CXCR4(R334X), a hyperfunctional mutant chemokine receptor and cause of WHIM syndrome. J Cell Mol Med 2011;15:2071–2081.

19 Kawai T, Choi U, Cardwell L et al. WHIM syndrome myelokathexis reproduced in the NOD/SCID mouse xenotransplant model engrafted with healthy human stem cells transduced with C-terminus-truncated CXCR4. Blood 2007;109:78–84.

20 Lagane B, Chow KY, Balabanian K et al. CXCR4 dimerization and beta-arrestin-mediated signaling account for the enhanced chemotaxis to CXCL12 in WHIM syndrome. Blood 2008;112:34–44.

21 Chung E, Hsu CL, Kondo M. Constitutive MAP kinase activation in hematopoietic stem cells induces a myeloproliferative disorder. PLoS One 2011;6:e28350.

22 Kuhn R, Schwenk F, Aguet M et al. Inducible gene targeting in mice. Science 1995;269:1427–1429.

23 Hamanaka S, Ooehara J, Morita Y et al. Generation of transgenic mouse line expressing Kusabira Orange throughout body, including erythrocytes, by random segregation of provirus method. Biochem Biophys Res Commun 2013;435:586–591.

24 Yamamoto R, Morita Y, Ooehara J et al. Clonal analysis unveils self-renewing lineage-restricted progenitors generated directly from hematopoietic stem cells. Cell 2013;154:1112–1126.

25 Sanuki S, Hamanaka S, Kaneko S et al. A new red fluorescent protein that allows efficient marking of murine hematopoietic stem cells. J Gene Med 2008;10:965–971.

26 Ema H, Morita Y, Yamazaki S et al. Adult mouse hematopoietic stem cells: Purification and single-cell assays. Nat Protoc 2006;1:2979–2987.

27 Osawa M, Hanada K, Hamada H et al. Long-term lymphohematopoietic reconstitution by a single CD34-low/negative hematopoietic stem cell. Science 1996;273:242–245.

28 Suzuki A, Obi K, Urabe T et al. Feasibility of ex vivo gene therapy for neurological disorders using the new retroviral vector GCDNsap packaged in the vesicular stomatitis virus G protein. J Neurochem 2002;82:953–960.

29 Nabekura T, Otsu M, Nagasawa T et al. Potent vaccine therapy with dendritic cells genetically modified by the gene-silencing-resistant retroviral vector GCDNsap. Mol Ther 2006;13:301–309.

30 Kawai T, Choi U, Whiting-Theobald NL et al. Enhanced function with decreased internalization of carboxy-terminus truncated CXCR4 responsible for WHIM syndrome. Exp Hematol 2005;33:460–468.

31 Morita Y, Ema H, Nakauchi H. Heterogeneity and hierarchy within the most primitive hematopoietic stem cell compartment. J Exp Med 2010;207:1173–1182.
32 Takano H, Ema H, Sudo K et al. Asymmetric division and lineage commitment at the level of hematopoietic stem cells: Inference from differentiation in daughter cell and granddaughter cell pairs. J Exp Med 2004;199:295–302.
33 Ogaeri T, Eto K, Otsu M et al. The actin polymerization regulator WAVE2 is required for early bone marrow repopulation by hematopoietic stem cells. Stem Cells 2009; 27:1120–1129.
34 Ploemacher RE, van der Sluijs JP, van Beurden CA et al. Use of limiting-dilution type long-term marrow cultures in frequency analysis of marrow-repopulating and spleen colony-forming hematopoietic stem cells in the mouse. Blood 1991;78:2527–2533.
35 Neben S, Anklesaria P, Greenberger J et al. Quantitation of murine hematopoietic stem cells in vitro by limiting dilution analysis of cobblestone area formation on a clonal stromal cell line. Exp Hematol 1993;21:438–443.
36 Dykstra B, Olthof S, Schreuder J et al. Clonal analysis reveals multiple functional defects of aged murine hematopoietic stem cells. J Exp Med 2011;208:2691–2703.
37 Bonig H, Priestley GV, Papayannopoulou T. Hierarchy of molecular-pathway usage in bone marrow homing and its shift by cytokines. Blood 2006;107:79–86.
38 Christopherson KW, 2nd, Hangoc G, Mantel CR et al. Modulation of hematopoietic stem cell homing and engraftment by CD26. Science 2004;305:1000–1003.
39 Hoggatt J, Singh P, Sampath J et al. Prostaglandin E2 enhances hematopoietic stem cell homing, survival, and proliferation. Blood 2009;113:5444–5455.
40 McCormick PJ, Segarra M, Gasperini P et al. Impaired recruitment of Grk6 and beta-Arrestin 2 causes delayed internalization and desensitization of a WHIM syndrome-associated CXCR4 mutant receptor. PLoS One 2009;4:e8102.
41 Bachelerie F. CXCL12/CXCR4-axis dysfunctions: Markers of the rare immunodeficiency disorder WHIM syndrome. Dis Markers 2010;29:189–198.
42 Levesque JP, Helwani FM, Winkler IG. The endosteal 'osteoblastic' niche and its role in hematopoietic stem cell homing and mobilization. Leukemia 2010;24:1979–1992.
43 Zlotnik A, Burkhardt AM, Homey B. Homeostatic chemokine receptors and organ-specific metastasis. Nat Rev Immunol 2011; 11:597–606.
44 Ema H, Takano H, Sudo K et al. In vitro self-renewal division of hematopoietic stem cells. J Exp Med 2000;192:1281–1288.
45 Umemoto T, Yamato M, Ishihara J et al. Integrin-alphavbeta3 regulates thrombopoietin-mediated maintenance of hematopoietic stem cells. Blood 2012;119:83–94.
46 Dar A, Kollet O, Lapidot T. Mutual, reciprocal SDF-1/CXCR4 interactions between hematopoietic and bone marrow stromal cells regulate human stem cell migration and development in NOD/SCID chimeric mice. Exp Hematol 2006;34:967–975.
47 Haribabu B, Richardson R, Fisher I et al. Regulation of human chemokine receptors CXCR4. Role of phosphorylation in desensitization and internalization. J Biol Chem 1997; 272:28726–28731.
48 Kawai T, Malech HL. WHIM syndrome: Congenital immune deficiency disease. Curr Opin Hematol 2009;16:20–26.
49 Chung SH, Seki K, Choi BI et al. CXC chemokine receptor 4 expressed in T cells plays an important role in the development of collagen-induced arthritis. Arthritis Res Ther 2010;12:R188.
50 Lapidot T, Kollet O. The essential roles of the chemokine SDF-1 and its receptor CXCR4 in human stem cell homing and repopulation of transplanted immune-deficient NOD/SCID and NOD/SCID/B2m(null) mice. Leukemia 2002;16:1992–2003.
51 Sharma M, Afrin F, Satija N et al. Stromal-derived factor-1/CXCR4 signaling: Indispensable role in homing and engraftment of hematopoietic stem cells in bone marrow. Stem Cells Dev 2011;20:933–946.
52 Kollet O, Spiegel A, Peled A et al. Rapid and efficient homing of human CD34(+)CD38(−/low)CXCR4(+) stem and progenitor cells to the bone marrow and spleen of NOD/SCID and NOD/SCID/B2m(null) mice. Blood 2001;97:3283–3291.
53 Cavazzana-Calvo M, Fischer A, Bushman FD et al. Is normal hematopoiesis maintained solely by long-term multipotent stem cells? Blood 2011;117:4420–4424.
54 Broxmeyer HE, Cooper S, Kohli L et al. Transgenic expression of stromal cell-derived factor-1/CXC chemokine ligand 12 enhances myeloid progenitor cell survival/antiapoptosis in vitro in response to growth factor withdrawal and enhances myelopoiesis in vivo. J Immunol 2003;170:421–429.
55 Porecha NK, English K, Hangoc G et al. Enhanced functional response to CXCL12/SDF-1 through retroviral overexpression of CXCR4 on M07e cells: Implications for hematopoietic stem cell transplantation. Stem Cells Dev 2006;15:325–333.
56 Lapidot T, Dar A, Kollet O. How do stem cells find their way home? Blood 2005;106: 1901–1910.

See www.StemCells.com for supporting information available online.

Leukemia (2014) **28**, 1844–1850

www.nature.com/leu

ORIGINAL ARTICLE

Haploinsufficiency of *Sf3b1* leads to compromised stem cell function but not to myelodysplasia

M Matsunawa[1,6], R Yamamoto[2,6], M Sanada[1,6], A Sato-Otsubo[1], Y Shiozawa[1], K Yoshida[1], M Otsu[2], Y Shiraishi[3], S Miyano[3,4], K Isono[5], H Koseki[5], H Nakauchi[2,7] and S Ogawa[1,7]

SF3B1 is a core component of the mRNA splicing machinery and frequently mutated in myeloid neoplasms with myelodysplasia, particularly in those characterized by the presence of increased ring sideroblasts. Deregulated RNA splicing is implicated in the pathogenesis of *SF3B1*-mutated neoplasms, but the exact mechanism by which the *SF3B1* mutation is associated with myelodysplasia and the increased ring sideroblasts formation is still unknown. We investigated the functional role of SF3B1 in normal hematopoiesis utilizing *Sf3b1* heterozygous-deficient mice. *Sf3b1*$^{+/-}$ mice had a significantly reduced number of hematopoietic stem cells ($CD34^-cKit^+Scal^+Lin^-$ cells or $CD34^-$ KSL cells) compared with *Sf3b1*$^{+/+}$ mice, but hematopoiesis was grossly normal in *Sf3b1*$^{+/-}$ mice. When transplanted competitively with *Sf3b1*$^{+/+}$ bone marrow cells, *Sf3b1*$^{+/-}$ stem cells showed compromised reconstitution capacity in lethally irradiated mice. There was no increase in the number of ring sideroblasts or evidence of myeloid dysplasia in *Sf3b1*$^{+/-}$ mice. These data suggest that *SF3B1* plays an important role in the regulation of hematopoietic stem cells, whereas *SF3B1* haploinsufficiency itself is not associated with the myelodysplastic syndrome phenotype with ring sideroblasts.

Leukemia (2014) **28,** 1844–1850; doi:10.1038/leu.2014.73

INTRODUCTION

Frequent pathway mutations involving multiple components of the RNA splicing machinery are a cardinal feature of myeloid neoplasms, particularly those showing myeloid dysplasia in which the major mutational targets include *SF3B1*, *U2AF1*, *SRSF2* and *ZRSR2*.[1–4] *SF3B1* mutations are one of the most common genetic alterations in myelodysplastic syndromes (MDS) and have also been reported in 5 – 15% of chronic lymphocytic leukemia cases,[5] and at lower frequencies in a variety of solid cancers such as endometrial cancers,[2] pancreatic carcinoma,[6] breast cancers[7] and uveal melanoma.[8] *SF3B1* mutations are considered to be one of the founding genetic events in MDS and define a benign clinical phenotype.[2,9] The frequency of *SF3B1* mutations is particularly high among the unique subtypes of MDS that are characterized by increased ring sideroblasts, such as refractory anemia with ring sideroblasts (RARS) or refractory cytopenia with multiple lineage dysplasia with ring sideroblasts as well as RARS associated with thrombocytosis[9,10] in which mutation frequencies of 66.7 – 79% have been reported. These genetic findings strongly suggest a close relationship between *SF3B1* mutation and the presence of ring sideroblasts. However, the molecular mechanism by which *SF3B1* mutation leads to myelodysplasia and promotes the formation of ring sideroblasts is unknown.

SF3B1 encodes subunit 1 of the splicing factor 3b complex that is a core component of U2 small nuclear ribonucleoprotein. The U2 small nuclear ribonucleoprotein complex recognizes the 3′ splice site at intron–exon junctions in normal pre-mRNA splicing machinery,[11] in which SF3B1 is involved in recognition of the branchpoint sequence. It has been demonstrated that *Sf3b1* knockout mice are embryonic lethal at very early stages, whereas *Sf3b1* heterozygous knockout (*Sf3b1*$^{+/-}$) mice exhibit mild skeletal alterations.[12] However, a detailed analysis of the functional role of *Sf3b1* in hematopoiesis in these mice has not been reported.

In this study we investigated the hematological phenotype of *Sf3b1*$^{+/-}$ mice to clarify the role of *SF3B1* in hematopoiesis and to obtain insights into how deregulation of *SF3B1* leads to the development of MDS phenotypes.

MATERIALS AND METHODS

Ethical approval of the study protocol

Animal experiments were undertaken with the approval of the Animal Care and Use Committee of the Institute of Medical Science, University of Tokyo (Tokyo, Japan).

Mice

Generation of *Sf3b1*$^{+/-}$ mice was as previously described.[12] C57BL/6(CD45.1$^+$) mice and C57BL/6 F1-CD45.1$^+$CD45.2$^+$ mice were purchased from Japan SLC (Shizuoka, Japan) and Sankyo-Lab Service (Tsukuba, Japan), respectively.

Iron staining

Prussian blue stain (Muto Pure Chemicals, Tokyo, Japan) and nuclear red counterstain with nuclear fast red were performed by standard procedures. Light microscopic images were acquired on an OLYMPUS BX45 microscope

[1]Departments of Pathology and Tumor Biology, Graduate School of Medicine, Kyoto University, Kyoto, Japan; [2]Division of Stem Cell Therapy, Center for Stem Cell Biology and Medicine, Institute of Medical Science, University of Tokyo, Tokyo, Japan; [3]Laboratory of DNA Information Analysis, Human Genome Center, Institute of Medical Science, The University of Tokyo, Tokyo, Japan; [4]Laboratory of Sequence Analysis, Human Genome Center, Institute of Medical Science, The University of Tokyo, Tokyo, Japan and [5]Laboratory for Developmental Genetics, RIKEN Research Center for Integrative Medical Sciences, Yokohama, Japan. Correspondence: Dr S Ogawa, Departments of Pathology and Tumor Biology, Kyoto University, Yoshida Konoe-cho, Sakyo-ku, Kyoto 606-8501, Japan.
E-mail: sogawa-tky@umin.ac.jp
[6]These authors contributed equally to this work.
[7]These authors jointly directed this work.
Received 27 January 2014; accepted 10 February 2014; accepted article preview online 18 February 2014; advance online publication, 25 March 2014

and an OLYMPUS DP25 camera using DP2-BSW software (version 2.2; Olympus, Tokyo, Japan).

Colony-forming assays

Bone marrow (BM) cells (2.5×10^4 cells) from *Sf3b1*$^{+/-}$ or *Sf3b1*$^{+/+}$ mice at the age of 8 weeks were seeded into methylcellulose-containing medium (MethoCult M3234; Stem Cell Technologies, Vancouver, BC, Canada) supplemented with 10 ng/ml murine interleukin-3, 10 ng/ml murine interleukin-6, 20 ng/ml murine thrombopoietin, 50 ng/ml murine stem cell factor (Wako Pure Chemical, Osaka, Japan) and 3 U/ml human recombinant erythropoietin (R&D Systems, Minneapolis, MN, USA). The number of colonies was counted after 14 days of culture.

Flow cytometry

Measurement of hematopoietic stem cells (HSCs) and hematopoietic progenitor cells was conducted in 8-week-old male mice as previously described.[13] Stained cells were analyzed with FACSAria II or FACSCanto II flow cytometers (BD Bioscience, Franklin Lakes, NJ, USA). Cell sorting was performed on a MoFlo system (Beckman Coulter, Fullerton, CA, USA). Data were analyzed by FlowJo software (Tree Star, Ashland, CA, USA). The antibodies used in this study are listed in the Supplementary Table 1.

Competitive repopulation assay

Unfractionated pooled BM cells (1×10^6 cells) from 8-week-old *Sf3b1*$^{+/-}$ or *Sf3b1*$^{+/+}$ mice (CD45.2$^+$) were transplanted into 8–12-week-old female CD45.1$^+$ recipient mice lethally irradiated at 2 doses of 4.9 Gy together with the same number of BM cells from 8–12-week-old male CD45.1$^+$/CD45.2$^+$ mice as competitors. Sorted 120 CD34$^-$KSL cells as well as 80 CD150$^+$CD34$^-$KSL cells obtained from *Sf3b1*$^{+/-}$ or *Sf3b1*$^{+/+}$ mice were transplanted into lethally irradiated recipients together with competitor whole BM cells (5×10^5 cells). At 40 weeks after transplantation, BM cells (1×10^7) were harvested from the recipient mice and were serially transplanted into second recipients. The chimerism of donor-derived cells was evaluated by flow cytometry as previously described.[14] The antibodies used in this study are listed in the Supplementary Table 1.

Gene expression analyses

Total RNA was prepared from CD34$^-$KSL cells, pooled from 3 female mice at the age of 11–13 weeks, using NucleoSpin RNA XS (Macherey-Nagel, Düren, Germany). For RNA sequencing analyses, the synthesis and amplification of complementary DNA was done using a SMARTer Ultra Low RNA kit for Illumina sequencing (Clontech Laboratories, Mountain View, CA, USA) according to the manufacturer's protocol. Sequencing libraries were generated using the NEBNext DNA Library Prep Reagent Set for Illumina (New England BioLabs, Ipswich, MA, USA) and analyzed using Illumina HiSeq 2000 (Illumina, San Diego, CA, USA) according to the manufacturer's protocol. Data processing was performed as described previously.[1,15] All sequence reads were mapped to the mouse transcriptome based on the UCSC known gene (downloaded in June 2013) using bowtie ver. 0.12.7 (http://bowtie-bio.sourceforge.net/index.shtml),[16] and unmapped or poorly mapped reads were realigned to mouse reference genome (mm10) using BLAT (http://genome.ucsc.edu/).[17] The expression level of each transcript was quantified with normalized fragments per kilobase of transcript per million fragments sequenced[18] that were calculated using bedtools ver. 2.17.0 (https://code.google.com/p/bedtools/)[19] with a transcriptome reference (RefSeq Genes, downloaded in June 2013). Gene set enrichment analyses (GSEA) were performed with GSEA[20] ver. 2.0.13 software from the Broad Institute (http://www.broad.mit.edu/gsea). For quantitative reverse transcriptase-PCR, RNA was subjected to reverse transcription using the ReverTra Ace qPCR RT kit (Toyobo, Osaka, Japan) according to the manufacturer's protocol. Quantitative expression levels of mRNA were measured as described previously.[1,15] Primers used for quantitative reverse transcriptase-PCR are listed in the Supplementary Table 2.

Statistical analyses

Statistical significance was evaluated by Student's *t*-test, and $P<0.05$ was considered significant.

Table 1. Peripheral blood counts of *Sf3b1*$^{+/+}$ and *Sf3b1*$^{+/-}$ mice at 8 weeks

Parameter	*Sf3b1*$^{+/+}$	*Sf3b1*$^{+/-}$	N	P-*value*
WBC count ($\times 10^4$/μl)	1.32 ± 0.56	1.09 ± 0.28	6	0.39
Neutrophil (%)	13.67 ± 6.40	15.83 ± 6.28	6	0.57
Lymphocyte (%)	80.58 ± 7.14	79.08 ± 6.50	6	0.71
Monocyte (%)	5.75 ± 1.54	5.08 ± 2.84	6	0.62
Hb level (g/dl)	18.23 ± 1.37	17.61 ± 1.00	6	0.39
PLT ($\times 10^4$/μl)	110.63 ± 22.68	119.30 ± 18.44	6	0.48

Abbreviations: Hb, hemoglobin; PLT, platelets; WBC, white blood cells. Data are the mean ± s.d. (n = 6).

RESULTS

Hematologic findings are not disturbed in *Sf3b1*$^{+/-}$ mice

No *Sf3b1*-null mice were obtained, confirming the previous observation that *Sf3b1*$^{-/-}$ mice should be embryonic lethal. However, *Sf3b1*$^{+/-}$ mice were obtained at an expected frequency compared with *Sf3b1*$^{+/+}$ littermates and appeared grossly normal.[12] The complete peripheral blood counts in *Sf3b1*$^{+/-}$ mice at 8 weeks of age were comparable with those in *Sf3b1*$^{+/+}$ littermate mice with normal differential counts of white blood cells (Table 1). There was no significant change in the peripheral blood counts between *Sf3b1*$^{+/+}$ and *Sf3b1*$^{+/-}$ mice at any time points up to 54 weeks (Supplementary Figures 1a and b). *Sf3b1*$^{+/-}$ mice did not show any significant differences in total BM cellularity or the number of megakaryocytes, and their lineage composition was comparable with that of *Sf3b1*$^{+/+}$ mice (Table 2). No splenomegaly was observed in any mice tested in these experiments, and spleen weights were also similar to those of *Sf3b1*$^{+/+}$ mice (Table 2). No significant morphologic abnormalities were recognized in peripheral blood and BM cells in May–Grünwald–Giemsa staining. Taken together, these findings suggested that steady-state hematopoiesis was maintained almost normally in *Sf3b1*$^{+/-}$ mice.

The number of ring sideroblasts is not increased in *Sf3b1*$^{+/-}$ mice

To determine whether loss of *Sf3b1* alone can lead to increased production of ring sideroblasts, we examined cytospin BM specimens by Prussian blue staining for iron. In contrast to the previous report describing increased formation of ring sideroblasts in the same *Sf3b1*$^{+/-}$ strain of mouse,[21] we observed very few sideroblasts characterized by nuclei encircled by a small number of iron granules. Specifically, there was no significant difference in the number of sideroblasts between *Sf3b1*$^{+/-}$ and *Sf3b1*$^{+/+}$ mice at 8 weeks (Figures 1a and b) and also at 54 weeks (Supplementary Figure 1c).

Decreased HSC fraction in *Sf3b1*$^{+/-}$ mice

We evaluated HSCs and progenitor cells by flow cytometric analyses to further assess the hematopoietic system in the BM of 8-week-old mice. Interestingly, the frequency and the absolute number of HSCs, defined as CD34$^-$/low c-Kit$^+$ Sca1$^+$ Lineage$^-$ (CD34$^-$ KSL),[22] were significantly decreased in *Sf3b1*$^{+/-}$ mice (Figures 2a–c). On the other hand, there were no significant differences in the number of hematopoietic progenitor cell fraction (CD34$^+$ KSL cells), megakaryocyte–erythroid progenitors, common myeloid progenitors or granulocyte–monocyte progenitors between *Sf3b1*$^{+/+}$ and *Sf3b1*$^{+/-}$ mice (Figures 2a–f). *SF3B1* mutations were also seen in a subset of chronic lymphocytic leukemia cases, but no obvious changes in the common lymphoid progenitor population in BM were observed (Figures 2g–i).

Table 2. Bone marrow cell counts and spleen size of $Sf3b1^{+/+}$ and $Sf3b1^{+/-}$ mice at 8 weeks

Parameter	$Sf3b1^{+/+}$	$Sf3b1^{+/-}$	N	P-*value*
Total nucleated cells ($\times 10^7$)	5.04 ± 1.62	6.20 ± 0.84	6	0.15
Myeloid (%)	65.42 ± 4.35	66.67 ± 4.36	6	0.63
Erythroid (%)	17.08 ± 4.34	12.58 ± 3.43	6	0.07
Lymphoid (%)	13.58 ± 3.17	18.33 ± 5.17	6	0.08
Monocyte (%)	3.92 ± 2.85	2.42 ± 1.88	6	0.31
Megakaryocyte (6×10^4 nucleated cells)	7.00 ± 2.00	8.33 ± 1.75	6	0.27
Spleen weight (mg)	54.64 ± 9.83	64.64 ± 14.10	6	0.24

Data are the mean ± s.d. ($n = 6$).

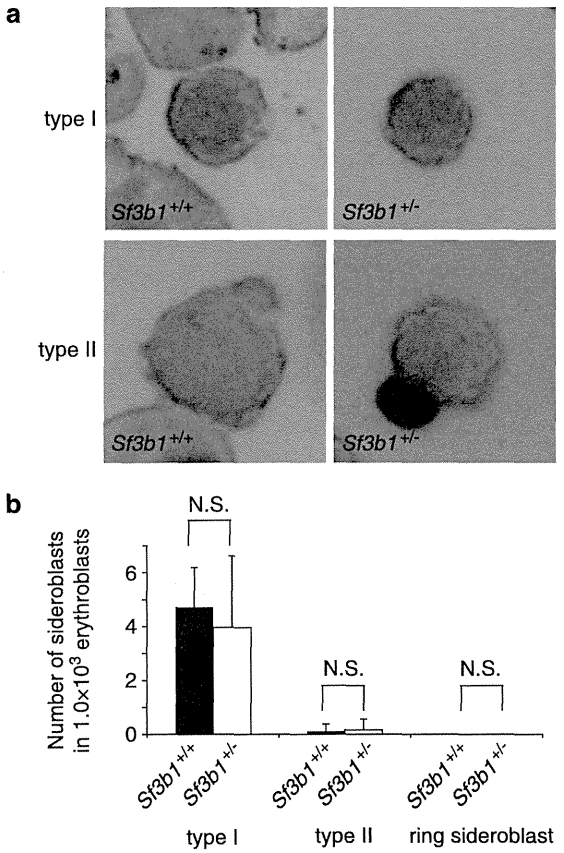

Figure 1. The number of sideroblasts is not increased in $Sf3b1^{+/-}$ mice. (**a**) Representative images of BM cytospin slides from $Sf3b1^{+/+}$ and $Sf3b1^{+/-}$ mice stained with Prussian Blue iron staining for the detection of sideroblasts. Sideroblasts were defined as follows: type I, sideroblasts with <5 siderotic granules in the cytoplasm; type II, sideroblasts with $\geqslant 5$ siderotic granules, but not in a perinuclear distribution; and ring sideroblasts with $\geqslant 5$ granules in a perinuclear position, surrounding the nucleus or encompassing at least one-third of the nuclear circumference. Original magnification $\times 1000$. (**b**) The number of cells with siderotic granules counted per 1.0×10^3 erythroblasts; $n = 6$ mice per genotype. Data represent the mean ± s.d. NS, not significant.

In addition, splenic B cell populations were not significantly changed between $Sf3b1^{+/+}$ and $Sf3b1^{+/-}$ mice (Supplementary Figures 2a and b).

Next, we performed *in vitro* colony-forming cell assays using whole BM cells. Consistent with the reduction in the HSC fraction in $Sf3b1^{+/-}$ mice, the number of hematopoietic colonies in $Sf3b1^{+/-}$ mice BM cells was significantly lower than that in $Sf3b1^{+/+}$ mice (Figure 3a). No significant differences in the distribution of colony size or colony types were observed. These data also suggested that haploinsufficiency of *Sf3b1* leads to a decrease in the number of HSCs/immature progenitor cells, although there was no significant difference in the numbers of differentiated or mature blood cells.

Reduced number and impaired function of HSCs in $Sf3b1^{+/-}$ mice

Next, we assessed the reconstitution capacity of total BM cells from $Sf3b1^{+/-}$ mice using competitive repopulation assays. In these assays, 1.0×10^6 total BM cells from $Sf3b1^{+/+}$ or $Sf3b1^{+/-}$ mice ($CD45.1^-/CD45.2^+$) were transplanted into lethally irradiated recipient mice ($CD45.1^+/CD45.2^-$) with the same number of competitor cells from $CD45.1^+/CD45.2^+$ $Sf3b1^{+/+}$ mice. Then, the chimerism of donor-derived $CD45.1^-/CD45.2^+$ cells in the peripheral blood of recipient mice was measured by flow cytometry up to 40 weeks after transplantation. The chimerism of $Sf3b1^{+/-}$-derived $CD45.1^-/CD45.2^+$ cells in peripheral blood was significantly lower than that of $Sf3b1^{+/+}$ derived cells (Figure 3b), suggesting the compromised hematopoietic repopulation capacity of $Sf3b1^{+/-}$ mice. To confirm this finding further, we performed competitive repopulation assays using purified HSC fractions ($CD34^-$ KSL cells; Figure 3b). Similar to the result of competitive reconstitution assay using whole BM cells, the chimerism of donor-derived $CD45.2^+$ cells in peripheral blood was also reduced in the mice transplanted with $Sf3b1^{+/-}$ mice-derived HSCs compared with that in mice transplanted with $Sf3b1^{+/+}$ mice-derived HSCs. These observations suggested that the HSCs from $Sf3b1^{+/-}$ mice had significantly reduced reconstitution capacity compared with those from $Sf3b1^{+/+}$ mice (Figure 3b). The lineage contribution of $Sf3b1^{+/-}$ cells in peripheral blood was comparable with that of $Sf3b1^{+/+}$ cells (Figure 3b). These findings were confirmed by competitive repopulation assays using enriched long-term HSCs ($CD150^+$ $CD34^-$ KSL cells; Figure 3c).[23,24]

Furthermore, we performed serial transplantation experiments of whole BM and HSCs to assess the long-term reconstitution capacity of $Sf3b1^{+/-}$ HSCs more precisely. $Sf3b1^{+/-}$ mice showed reduced chimerism of donor-derived $CD45.2^+$ cells in the primary transplantations of competitive whole BM and competitive HSCs, and the reduced chimerism was even more pronounced after secondary transplantations (Figure 3d). In summary, HSCs in $Sf3b1^{+/-}$ mice reduce not only their number but also their competitive repopulation capacity of hematopoiesis.

The effect of *Sf3b1* haploinsufficiency on gene expression

To investigate the molecular mechanisms of the impaired function of HSCs induced by *Sf3b1* haploinsufficiency, we conducted gene expression analyses by RNA sequencing using $CD34^-$KSL cells isolated from $Sf3b1^{+/-}$ and $Sf3b1^{+/+}$ mice (Supplementary Table 3). Differentially expressed genes in $Sf3b1^{+/-}$ mice, including 1059 upregulated and 828 downregulated genes, from those of